Soil Salinity Detection Using Satellite Remote Sensing

Fouad Al-Khaier
March, 2003

Soil Salinity Detection Using Satellite Remote Sensing

by

Fouad Al-Khaier

Thesis submitted to the International Institute for Geo-information Science and Earth Observation in partial fulfilment of the requirements for the degree of Master of Science in

Geo-information Science and Earth Observation,
Watershed Management, Conservation and River Basin Planning specialization.

Degree Assessment Board

Ir. A.M. van Lieshout (Chairman) WRS Department, ITC
Dr. Ir. M.G. Bos (External Examiner) ILRI-Alterra, Wageningen
Prof. Dr. W.G.M. Bastiaanssen (Supervisor) WRS Department, ITC
Dr. A.S.M. Gieske (Member) WRS Department, ITC

INTERNATIONAL INSTITUTE FOR GEO-INFORMATION SCIENCE AND EARTH OBSERVATION
ENSCHEDE, THE NETHERLANDS

Disclaimer

This document describes work undertaken as part of a programme of study at the International Institute for Geo-information Science and Earth Observation. All views and opinions expressed therein remain the sole responsibility of the author, and do not necessarily represent those of the institute.

وَفَوْقَ كُلِّ ذِي عِلْمٍ عَلِيمٌ ..

إلى روح أبي الطاهرة..

Acknowledgments

I owe a dept of gratitude to the Netherlands government and to the International Institute for Geo-information Science and Earth Observation ITC, for giving the opportunity to follow the MSC course in the Netherlands through the Netherlands fellowship program.

I am greatly indebted to Prof. Dr. W.G.M. Bastiaanssen whom without his great effort and guidenss this study would not see the light. I would like to thank Ir. A.M. van Lieshout for his guidance and great support throughout my study. Many thanks to Messrs: Prof. A.M.J. Meijerink, Dr. A.S.M. Gieske, Dr.Ir. Chris Mannaerts, Ir. Gabriel Norberto Parodi, Dr. Zoltan Vekerdy, Drs. Robert Becht and Ing. Remco Dost to their unlimited support and encouragement during the study period.

I am greatly indebted to Ing. kaees Al-Assad who has a great rule in my following this course in the Netherlands. Many thanks to Ing. Tareef Al-Naeif who was of great help and support during the field work. I would like to thank also Ing Hassan Al-Eeisa who was great friend during the fieldwork.
I wish to thank my sincere friend Nizar Hag_Ahmad for his continuous moral support and encouragement. Also I wish to thank my friend Chaweepan Suangkiattikun who is a very precious friend and forever.

I do gratefully thank my parents in law for their supporting and encouragement. Finally it is hardly possible to find appropriate words to express my gratefulness to my wife Ashwak and my daughter Leen. I am deeply indebted to them for the time both I could not spend with them.

Abstract

Remote sensing has been shown to be a particularly valuable tool for obtaining relevant data on soil salinity in the irrigated area. The presence of salts at the terrain surface can be detected from remotely sensed data either directly on bare soils, with salt efflorescence and crust, or indirectly through the biophysical characteristics of vegetation as these are affected by salinity.

This study dealt with the two different methods (empirical and biophysical) using two different types of satellite data (Landsat7 ETM and ASTER) in two different crop calendar dates (immediately before the growing season and in the middle of it).

The first method, the empirical, which conducted on an image of the newly launched ASTER sensor, resulted in two indexes,

- The Salinity index, which is produced by ASTER bands: $\left(\frac{band4 - band5}{band4 + band5}\right)$ (has an accurate detection for overall salinity in the bare agriculture soils. This can be applied when the land is fallow.
- The index, which is produced by ASTER bands: $\left(\frac{band4 - band3}{band4 + band3}\right)$ has the potential to detect the chemical soil composition such as nitrogen or iron dioxides. More research is required to prove this statement

The second method the biophysical method which needs to be applied during the growing season. The method is based on detecting the crop reaction to soil salinity via the osmotic forces and the increasing surface resistance due to stomatal closure.

The relationship between the surface resistance of cotton (calculated from a Landsat Enhanced Thematic Mapper image using the SEBAL method) and the EC obtained in the field. is encouraging (R^2=0.86). When other factors like water stress play no role, calculating r_s from the satellite images in the middle of the growing season gives us a fair idea about soil salinity in the upper 0.75 cm of the soil column

Table of Contents

List of Figures

List of Tables

List of Appendices

Chapter 1 Introduction

1.1. Introduction

The introduction of irrigation into the arid regions of many countries has caused the loss of large areas of formerly productive lands through water logging and salinization (Afghanistan, Pakistan, Syria, China). This degradation is caused not by the process of irrigation itself, but by its incorrect or careless application, and measures are now being successfully applied for the reclamation of some areas (Pakistan, China).

In fact the irrigation development in the arid zone almost always has to deal with not only secondary but also with primary and fossil salinity. This primary and fossil salt mobilization has been found to be one of the principal causes of the river's salinization in irrigated basins in the arid zone (Smedema and Shiati, 2002).

The importance of land in the Syrian Arab Republic appears from the fact that the national gross income depends on agricultural production. More than 65% of the Syrian population depends on agricultural production and land exploitation to earn their living.

Being aware of this fact, the Syrian government over the last three decades has provided means to modernize the agricultural technology to exploit the land and water resources better. Meanwhile, some problems have come to the surface such as deterioration of the environment.

In the fifties, growing cotton widely spread in Syria due to its high profit, Syrian farmers rushed to exploit the land to its maximum capacity without considering the sustainability of the agricultural production of the land, neither the potential of applying the drainage systems nor maintaining them when available. Salt affected areas have now mastered a large part of the basins Euphrates, Khaboor and Balikh.

Salinization has become the most threatening problem that faces agriculture in Syria as it has started to spread in some areas since 1980s, and it will affect the livelihood of rural people.

1.2. **Soil Salinity**: definition, distribution and causes

Soil salinity, as a term, that refers to the state of accumulation of the soluble salts in the soil. Soil salinity can be determined by measuring the electrical conductivity of a solution extracted from a water-saturated soil paste. The electric conductivity as EC_e (Electrical Conductivity of the extract) with units of decisiemens per meter ($dS.m^{-1}$) or millimhos per centimetre (mmhos/cm) is an expression for the anions and cations in the soil.

From the agricultural point of view, saline soils are those, which contain sufficient neutral soluble salts in the root zone to adversely affect the growth of most crops (see table 1.1). For the purpose of definition, saline soils have an electrical conductivity of saturation extracts of more than 4 $dS.m^{-1}$ at 25 °C (Richards, 1954).

Table 1.1 General ranges for plant tolerance to soil salinity.

Salinity (EC_e, $dS.m^{-1}$)	Plant response
0 to 2	Mostly negligible
2 to 4	growth of sensitive plants may be restricted
4 to 8	growth of many plants is restricted
8 to 16	only tolerant plants grow satisfactorily
above 16	only a few, very tolerant plants grow satisfactorily

As salinity levels increase, plants extract water less easily from soil, aggravating water stress conditions. High soil salinity can also cause nutrient imbalances, which then result in the accumulation of elements toxic to plants, and reduce water infiltration if the level of one salt element (like sodium) is high. In many areas, soil salinity is the factor limiting plant growth. Table 1.2 shows the salinity tolerance of some kinds of crops.

Table 1.2. Salinity tolerance of some kinds of crops

Crop	Threshold value	10% yield loss	25% yield loss	50% yield loss	100% yield loss
	EC_e ($dS.m^{-1}$)	EC_e ($dS.m^{-1}$)	EC_e ($dS.m^{-1}$)	EC_e ($dS.m^{-1}$)	EC_e ($dS.m^{-1}$)
Beans (field)	1.0	1.5	2.3	3.6	6.5
Cotton	7.7	9.6	13.0	17.0	27.0
Maize	1.7	2.5	3.8	5.9	10.0
Sorghum	4.0	5.1	7.2	11.0	18.0
Sugar beets	7.0	8.7	11.0	15.0	24.0
Wheat	6.0	7.4	9.5	13.0	20.0

adapted from Doorenbos and Kassam (1979)

There are extensive areas of salt-affected soils on all the continents, but their extent and distribution have not been studied in detail (FAO, 1988). In spite of the availability of many sources of information, accurate data concerning salt affected lands of the world are rather scarce (Gupta and Abrol, 1990).

Statistics relating to the extent of salt-affected areas vary according to authors, but estimates are in general close to 1 billion hectares (see table 1.3), which represent about 7% of the earth's continental extent (Ghassemi, Jakeman, and Nix, 1995). In addition to these naturally salt-affected areas, about 77 M ha have been salinized as a consequence of human activities, with 58% of these concentrated in irrigated areas. On average, salts affect 20% of the world's irrigated lands, but this figure increases to more than 30% in countries such as Egypt, Iran and Argentina (Ghassemi, Jakeman, and Nix, 1995).

Table 1.3 Extent of salt-affected soils (Szabolcs, 1979).

Region	Million of hectares
North America	15.7
Mexico and Central America	2.0
South America	129.2
Africa	80.5
South Asia	84.8
North and Central Asia	211.7
Southeast Asia	20.0
Australia	357.3
Europe	50.8
Total	**952.0**

According to estimates by FAO and UNESCO, as much as half of the world's existing irrigation schemes is more or less under the influence of secondary salinization and waterlogging. About 10 million hectares of irrigated land are abandoned each year because of the adverse effects of irrigation, mainly secondary salinization and alkalinization (Szabolcs, 1987). Figure 1.1 shows an estimation of the global distribution of salt-affected areas

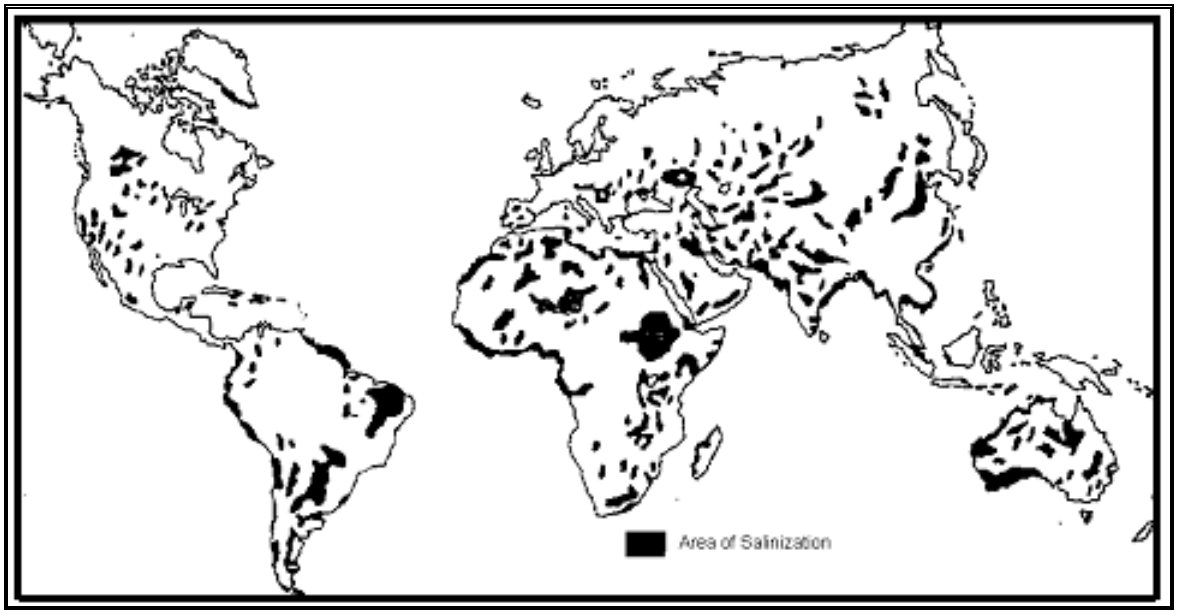

Figure 1.1 Global distributions of salt-affected soils (Szabolcs, 1985).

In spite of the general awareness of these problems and past sad experiences, salinization and waterlogging of irrigated land continue to increase. In some countries, land salinization may even threaten the national economy. It is particularly series issues in Argentina, Egypt, India, Iraq, Pakistan, Syria and Iran (Rhoades, 1990).

Saline soils may occur in any region and under every climate in the world. However, these soils are mostly concentrated in semi-arid and arid regions. One of the conditions for the presence or formation of saline soils is an evaporation, which greatly exceeds the precipitation.

The sources of salt in the soil may vary:

1. The salt can be present in the parent material, e.g., in salt layers, accumulated in earlier times. This form may be present in the Balikh basin in some gypsiferous deposits, and deeper formations, origination from the era in which the extension of the Arabian Gulf became land in the Mesopotamian depression.
2. The salt can be formed during weathering of the parent rock. Salts are generally set free by rock weathering but they will be leached, as this process is very slow. However, some kinds of rock have a chemical composition and porous texture so that under warmer climates relatively high proportions of salts are formed.
3. The salt can be air borne. In this case it is transported through the air by dust or by rainwater. In the Euphrates valley transport of salt by dust is common phenomenon, but it has local importance.
4. The ground water can be saline. This may originate from reasons mentioned above. In this case where the water table is near to the surface, salt will accumulate in the topsoil as a result of the evaporation. When the water table occurs deeper in the soil, the saline layer can be formed at some depth, which may influence the soil after use, especially with uncontrolled irrigation and inadequate drainage practice. In the Euphrates valley and at other places in Balikh, the ground water table is near to the surface during part of the year so the salt accumulation is present and even salt crusts are formed. In particular the drainage water in gypsiferous areas contributes to the salinization.
5. Salt brought by irrigation water. Irrigation water always contains some salt and incorrect methods may lead to accumulation of this salt. When waterlogging is present at some depth the water evaporates again and the salt transported with the water from elsewhere is left behind.

In principle, soil salinity is not difficult to manage. The first prerequisite for managing soil salinity is adequate drainage, either natural or man-made. If the salinity level is too high for the desired vegetation, removing salts is done by leaching the soil with clean (low content of salts) water. Application of 6 inches of water will reduce salinity levels by approximately 50%, 12 inches of water will reduce salinity by approximately 80%, and 24 inches by approximately 90%.

The manner in which water is applied is important. Water must drain *through* the soil rather than run off the surface. Internal drainage is imperative and may require deep tillage to break up any restrictive layer impeding water movement. Sprinkler irrigation systems generally allow better control of water application rates; however, flood irrigation can be used if sites are level and water application is controlled.

However, the determination of when, where and how salinity may occur is vital to determining the sustainability of any irrigated production system. Remedial actions require reliable information to help set priorities and to choose the type of action that is most appropriate in each

case. Decision-makers and growers need confidence that all technical estimates and data provided to them are reliable and robust, as the economic and social effects of over- or underestimating the extent, magnitude, and spatial distribution of salinity can be disastrous (Metternicht and Zinck, 2003).

To keep track of changes in salinity and anticipate further degradation, monitoring is needed so that proper and timely decisions can be made to modify the management practices or undertake reclamation and rehabilitation. Monitoring salinity means first identifying the places where salts concentrate and, secondly, detecting the temporal and spatial changes in this occurrence. Both largely depend on the peculiar way salts distribute at the soil surface and within the soil mantle, and on the capability of the remote sensing tools to identify salts (Zinck, 2001).

Irrigation-induced water logging and salinization are highly dynamic conditions, which vary widely in time and in space. The development of reliable, easy-to-use, low-cost remote sensing methods for monitoring and mapping of water logging and salinity conditions in irrigated areas would give the concererned countries a very valuable tool in the combat of salinity control of irrigated land (Smedema, 1993).

1.3. Literature review

Remote sensing performs the detection, collection and interpretation of data from distance by mean of sensors. The sensors measure the reflectance of electromagnetic radiations from the features at the earth surface. The radiation energy is transmitted through space in waveform and is defined by wavelength and amplitude or oscillation. The electromagnetic spectrum ranges from gamma rays, with wavelength of less than 0.03 nm, to radio energy with a wavelength of more than 30 cm. In remote sensing applied to land resources surveys, wavelengths between 0.4 and 1.5 mm are commonly used.

A variety of remote sensing data has been used for identifying and monitoring salt-affected areas, including aerial photographs, video images, infrared thermography, visible and infrared multispectral and microwave images (Metternicht and Zinck, 2002).

The use of the multispectral scanning (MSS) technology for natural resource surveys concerns the images obtained by Landsat MSS/TM (Thematic Mapper) and Spot. Type and variation of the images depend on the electronic scanners, which record the reflected radiations in the separate bands. Landsat offers a much wider rang of bands (spectral diversity) than SPOT, which enhance the detection of surface features.

Both types of classification, unsupervised and supervised, were used for the proper identification of salinity, mostly at regional level. MSS bands 3, 4 and 5 are recommended for salt detection in addition to TM bands 3, 4, 5 and 7 (Naseri, 1998).

Interesting studies of using satellite images for salinity detection were conducted by Chaturvedi et al. (1983) and Singh and Srivastav (1990) using microwave brightness and thermal infrared temperature synergistically. The interpretation of the microwave signal was done physically by means of a two-layer model with fresh and saline groundwater.

Menenti, Lorkeers and Vissers (1986) found that TM data in bands 1 through 5 and 7 are good for identifying salt minerals, at least when they are a dominant soil constituent. Moreover, salt minerals affect the thermal behavior of the soil surface.

Mulders and Epema (1986) produced thematic maps indicating gypsiferous, calcareous and clayey surfaces using TM bands 3,4 and 5.They found that TM is valuable aid for mapping soil in arid areas when used in conjunction with aerial photographs.

Sharma and Bhargava (1988) followed a collative approach comprising the use of Landsat2_MSS "FCC"(False Colour Composite), survey of Topomaps and limited field checks for mapping saline soils and wetlands. Their results showed that because of their distinct coloration and unique pattern on false color composite imageries the separation of saline and waterlogged soil is possible.

Saha, Kudrat, and Bhan (1990) used digital classification of TM data in mapping salt affected and surface waterlogged lands in India, and found that these salt-affected and waterlogging areas could be effectively delineated, mapped and digitally classified with an accuracy of about 96 per cent using bands 3,4,5, and 7.

Rao et al. (1991) followed a systematic visual interpretation approach using FCC of TM bands 2,3 and 4 in the sake of mapping two categories, moderately and strongly sodic soils.

Steven et al. (1992) confirmed that near to middle infrared indices are proper indicators for chlorosis in the stressed crops (normalized difference for TM bands 4 and 5).

Mougenot and Pouget (1993) have applied thermal infrared information to detect hygroscopic characteristic of salts, and they found that reflectance from single leaves depends on their chemical composition (salt) and morphology.

The investigations of Vidal et al. (1996) in Morocco and Vincent et al. (1996) in Pakistan are based on a classification-tree procedure. In this procedure, the first treatment is to mask vegetation from non-vegetation using NDVI. Then the brightness index is calculated to detect the moisture and salinity status on fallow land and abandoned fields.

Dwivedi (1969) applied the principal component analysis of Landsat MSS bands 1, 2; 3and 4 in delineating salt affected soils.

Brena, et al. (1995), in Mexico, made multiple regression analysis using the electrical conductivity values and the spectral observations to estimate the electrical conductivity for each pixel in the field based on sampling sites. They generated a salinity image using the regression equation and the salinity classifications. And their experimental procedure was applied to an entire irrigation district in northern Mexico.

Ambast et al. (1997) used a new approach to classify salt affected and water logging areas through biophysical parameters of salt affected crops (albedo, NDVI), his approach based on energy partitioning system named Surface Energy Balance Algorithm For Land, SEBAL (Bastiaanssen, 1995).

It is clear that most of the published investigations based on remote sensing distinguish only three to four classes of soil salinity. Moreover most of them focused on empirical methods by a simple combination of multi spectral bands, and very few concentrated on the biophysical characteristics of the plants. These parameters that remote sensing has proved to give accurate measurements for.

Another remark can be made that the newly launched ASTER sensor with its variable spectral bands was not used for salinity detection yet.

1.4. Research Objectives

This study focuses on two major aspects:

- Exploring the potential of ASTER bands in mapping salinity, according to the temporal relationship between salt in the soil before planting and the growth of crops.

- Testing a new biophysical approach, by connecting the concept of surface resistance for a crop –in the case-"cotton" to the salinity of the soil.

1.5. Research hypotheses

This study has been built on three hypotheses:

1. Soil salinity affects the surface reflectance during the fallow period.
2. There should be a relationship between reflectance of bare soil in the fallow period and the cotton production.
3. There is a relationship between the surface resistance of a crop and the salinity of the soil on theoretical grounds, and thus there is a possibility to find out the location and the severity of soil salinity in the root zone

1.6. Outline Of The Thesis

Chapter 2 gives a general description of the study area and its features.

Chapter 3 describes the available data and materials, which have been collected through out the fieldwork, the satellite images which have been used, beside all the necessary processing that has been conducted on them.

Chapter 4 introduces the methods applied on both the Landsat image and ASTER image in order to detect salinity; two methods were distinguished and described:

- The empirical approach on the ASTER image: The applied methodology was described.

- The biophysical approach on Landsat image: the surface resistance concept is described and the relation between the surface resistance and soil salinity is demonstrated. A brief description of Surface Energy Balance Algorithm For Land, SEBAL is provided.

Chapter 5 presents the results obtained, from applying both methods.

Chapter 6 concludes the findings of this study, and gives some recommendations and opportunities for further research.

Chapter 2 Study Area Description

2.1 Geographical Information

The Balikh basin is located in the northern part of Syria (figure 2.1), with a total area of 370 km^2. The basin lies east of Euphrates reservoir. The water to the Balikh basin comes from the Euphrates reservoir. The study area lies between longitude 38º 43´ to 39º 03´ E and latitude 35º 55´ to 36º 13´ N. The study area is roughly triangular by the Euphrates on the south and by high land to the northwest and northeast. The river Balikh runs in from the north to join the Euphrates near Raqqa.

The agro-ecological conditions are very uniform over the whole project area; climate, topography, geology and soils are similar.

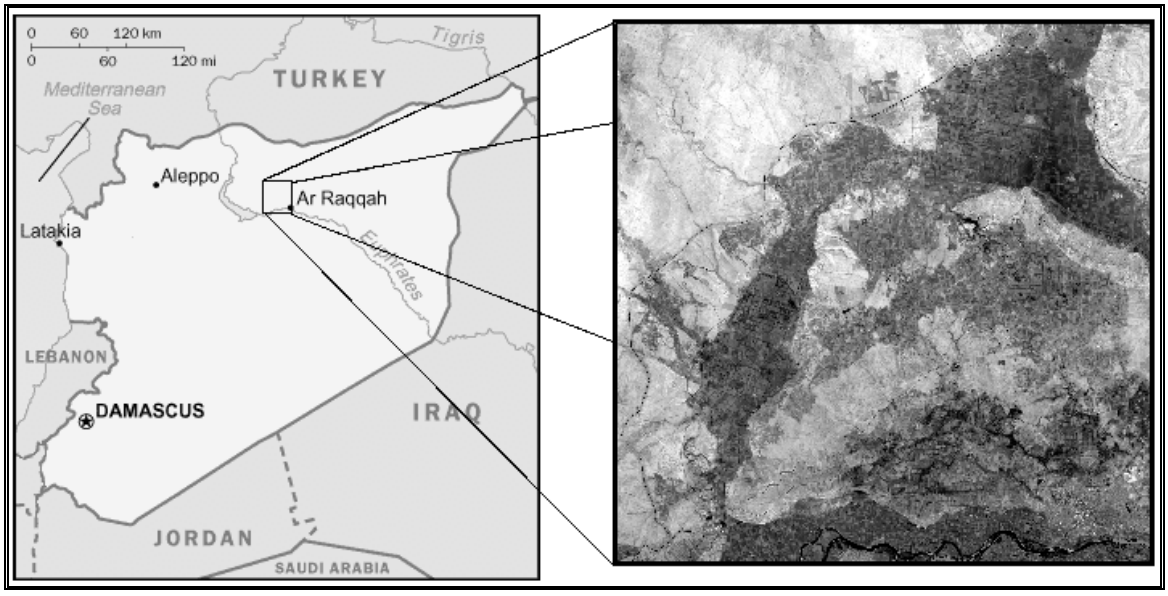

Figure 2.1 Location of the study area "Balikh basin" in Syria

2.2 Historical information

Along with the investigation on the construction Euphrates dam, many companies have studied this area for construction a complete irrigation scheme: irrigation canals, pumping stations, levelling, and drainage network have been created some 30 years ago. Among those companies are: Nedeco (The Netherlands) 1963, Sir Alexander Gibb and Partners (England) 1966, and Sogeria (France) 1976.

The project of reclaiming these lands started in 1970, and since accomplishing the dam (in 1973) the area has entered into service. The entire area is now under service by canals and drainage systems, however the performance is poor in some parts.

2.3 Climate

General

The climatological information shows that the conditions across the Balikh basin are fairly uniform. In the winter, rainfall in the northern area is higher than near the river Euphrates. However, the lack of summer rainfall and the uniform yearly temperature, humidity and evaporation ensure that, as far as climatological conditions are concerned, the entire study area can be considered as being climatologically homogeneous. (See table 2.1).

Precipitation

The rainfall from May up to and including October is very low and uniform for the study area. The increase in the total yearly rainfall in the northern corner occurs during the wintertime. This means that summer crops in the entire area are dependent on irrigation.

Temperature

The temperature also has a very small variation. The average amplitude of the temperature in July is 30°C plus or minus 9°C and in January (wintertime in Syria), about 7°C plus or minus 5°C.

Evaporation and Sunshine period

Evaporation in the region seems to be uniform, and high, with maximum of 12 to 13 mm daily during summer period. The data on sunshine show a very long duration of sunshine during the warm half of the year.

Humidity

The humidity shows a marked seasonal difference between summer and winter, but still it is rather uniform in the area.

Table 2.1 Monthly average meteorological data at Al-Raqqa station.

	Jan	Feb	Mar	Apr	May	Jun	Jul	Aug	Sep	Oct	Nov	Dec
Precipitation, mm	40.7	24.7	26.7	26.3	11.1	5.7	0.0	0.0	2.8	5.0	15.1	24.5
Wind velocity, $m.s^{-1}$ (10 m level)	2.8	2.9	3.4	3.3	3.7	4.9	6.0	4.8	3.6	2.2	2.0	2.4
Temperature, °C	6.6	8.7	12.7	17.5	23.3	28.1	30.0	29.0	25.2	19.7	13.4	8.5
Free water surface evaporation, mm (Average daily)	1.4	2.2	4.3	6.3	8.6	13.2	14.3	12.2	8.4	5.3	3	1.9
Relative humidity, %	79.0	71.0	59.0	54.0	40.0	33.0	38.0	39.0	42.0	47.0	62.0	75.0

2.4 Soils and salinity

The fieldwork shows a high uniformity of the texture in the upper section of the soil as the silty clay is covering the majority of the fields. In places gypsum is observed in the deeper subsoil.

In Euphrates valley, the ground water table is near to the surface during part of the year so that salt accumulation is present and even salt crusts are formed. In the balikh region in the deeper subsoil, certainly there are accumulations of salt (Paton and Mangnall, 1976).

2.5 Crops

The main crop cultivated is cotton, and is often planted in rotation with wheat. The following cropping systems can be observed (figure 2.2):

1. Cotton, not in rotation;

2. Cotton in the first year, immediately followed by wheat in the autumn. After harvesting the wheat in the spring the land is left fallow till the third year when cotton is planted again (2 years rotation);

3. Wheat in the first year. The land then is left fallow for the rest of the year and the next year till autumn when wheat is planted again (2 years rotation);

4. Cotton in the first year. The land thereafter is fallow for one year till next autumn when wheat is planted. After the harvesting of the wheat, the land is left fallow for another year and in the spring of the forth year cotton is planted (3 years rotation);

In addition to wheat, barley is often grown to provide grazing for sheep.

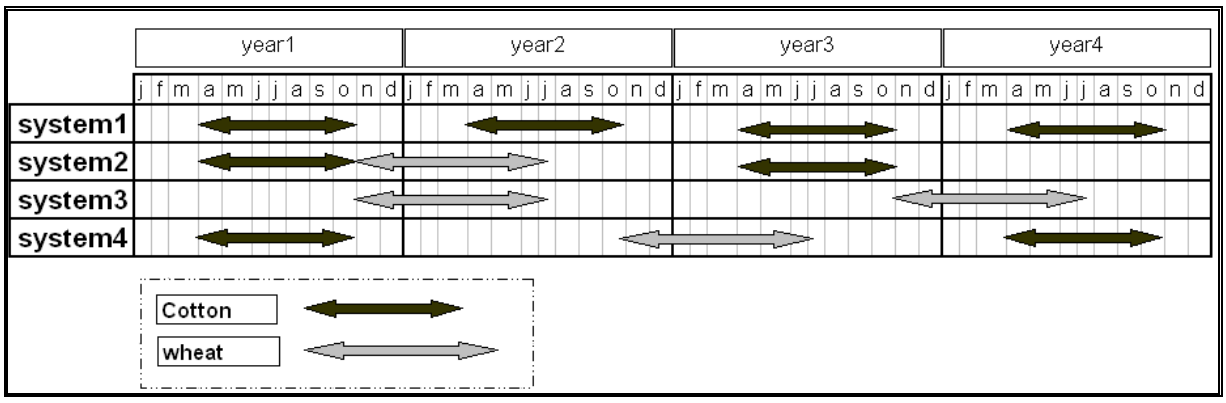

Figure 2.2 Difference of cropping systems in the area.

2.6 Irrigation

Due to the lack of rain the whole area is served by irrigation canals that reach all the fields by gravity, all the fields are irrigated by the flood method.

The main source of irrigation water is Euphrates, which classed as C2_S1 according to the U.S. salinity laboratories (Richard, 1954).
C2_water in conductivity class c2 can be used for irrigation plants. S1_Low sodium water can be used on almost all soils with little danger of accumulation of harmful amount of exchangeable sodium.

Chapter 3 Materials

3.1 Field collected data:

The field work took place in the period from August 22nd 2002 until October 4th 2002. The time was chosen to be in the middle of the growing season of cotton (end of March till mid of October), and about the time of Landsat image capturing, which planned to be taken in August 22nd 2002. The following materials were collected during the field visits,

Soil samples for ECe and PH measurements:

To cover the study area with a representative set of sample points, a day to day plan was made before going out to the fields. A hard copy of the ASTER image, which was taken on 10th March 2002, was used for choosing randomly the location of sampling points. The distance between sampling sites was approximately 1.5 to 2 km. The exact position of sampling points in latitude and longitude was identified by GPS (Global Positioning System). The depth and number of samples were determined according to the position of each point. Figure 3.1 shows the distribution of the sample points over the study area.

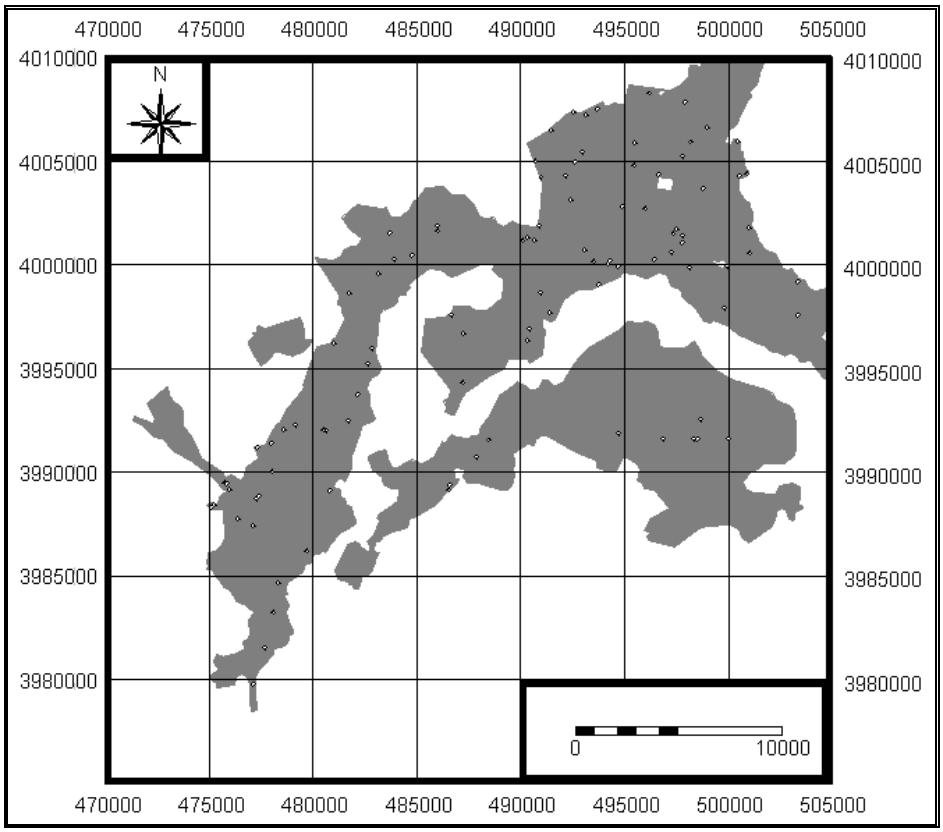

Figure 3.1 Distribution of the sample points over the study area.

- When the point was located in a bare land one sample from the upper layer (5-10) cm was to be taken.
- When the point inside a cotton field, three samples were to be taken at three depths: (5-10), (40-50), and (50-60) cm.

A total number of 98 points and 200 samples (see Appendix C) were collected. Figure 1 shows the distribution of these points in the study area.
The soil was dug by an auger, and kept in plastic bags labelled relevantly.

Soil analysis

The samples were sent to Al-Thawra laboratory where the method of soil salinity assessment (Rhoades et al, 1990) was applied to verify EC and pH. (see Appendix A)

Since the proportion of soil and distilled water was 1 to 5, the EC for this water extract is called EC5. The electrical conductivity of the saturated soil-paste extract (ECe) is then obtained by applying the formulas of Table 3.1, which have been produced by the Syrian field expertise in this particular region. (see Appendix D)

Table 3.1 Transferring EC5 To ECe from the field experiments with a correlation coefficient R2=0.9

EC5	The formula
Less than 1.4 $dS.m^{-1}$	ECe=EC5*4+0.45
More than 1.4 $dS.m^{-1}$ and less than 2.5 $dS.m^{-1}$	ECe=EC5*5.5
More than 2.5 $dS.m^{-1}$	ECe=EC5*6.4

Soil samples for calculating soil water content

The soil samples, which were used to verify soil moisture, were collected simultaneously with those used to verify EC, and had the same number, position, and depth.

Special care was taken to keep the soil moisture as it was in the field. That's why it was kept in soil sample rings (metal ring with cover), which covered tightly and wrapped outside with vinyl tape to prevent the loss of moisture. The gravimetric method has been applied (see Appendix B).

Water samples from the drain lines

Water samples were collected from some positions from the drain lines to get an idea about the EC in drained water from the fields.

Land cover points with GPS

When setting a land cover map it was necessary to take many GPS points of different features. GPS points from the borders ' corners' of the cotton fields were taken with special concentration.

Other features were located and marked by GPS points like the salt-crust and the water logging areas, poplar fields, maize fields, vegetable fields, etc.

Beside that GPS points were taken at road crossing, canal crossing, etc. to help create coordinate system and Georeferencing.

Remarks and photos

Observations and remarks about the crop health stage and appearance of salt (if it did exist) were necessary to take, as they have great value when compared with the satellite results after leaving the fieldwork.

3.2 Meteorological data

The meteorological data has been collected from three stations, which surrounded the study area from east, south and north. Namely: Al-thawra station, Al-Raqqa and Tall-Abiad (Figure 3.2). Table 3.2 shows the coordinates of these three stations.

Table 3.2 The coordinate of the meteorological stations

Station	Latitude	Longitude	Elevation (above sea level)	X (UTM) m	Y (UTM) m
Al-Thawra	**35º 51´ 00″ N**	**38º 32´ 24″ E**	**345m**	**458485**	**3967430**
Al-Raqqa	**35º 57´ 52″ N**	**39º 00´ 16″ E**	**251m**	**500069**	**3978635**
Tall-Abiad	**36º 42´ 22″ N**	**38º 57´ 96″ E**	**355 m**	**495815**	**4061690**

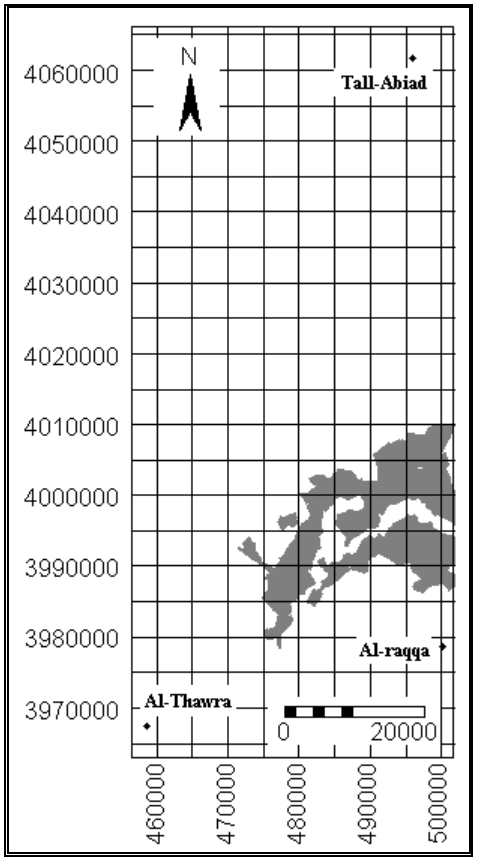

Figure 3.2 Location of the three stations.

The data were collected for the two days of taking ASTER images and Landsat images on 10th March 2002 and 24th August 2002 respectively.
The data are as following:

- Temperature, Relative humidity, Pressure, wind speed and direction every half an hour, from Al-Raqqa station.
- Wet temperature, dry temperature, dew point, Relative humidity, evaporation per day and soil temperature at different depths from the three stations and on 3 to 6 hour bases.

3.3 Office collected data

Many data has been collected from the offices of the institutes that are in charge of monitoring this area, like:

- Water table depths of the about 200 piezometers that spread in the area (Figure 3.3). And that is for the following periods (see Appendix E)
  - November 2000
  - January 2001
  - August 2001
  - May2002
  - July 2002
- Maps for the executed irrigation canals and drain lines in the area
- Reports and studies about salinity in the region.

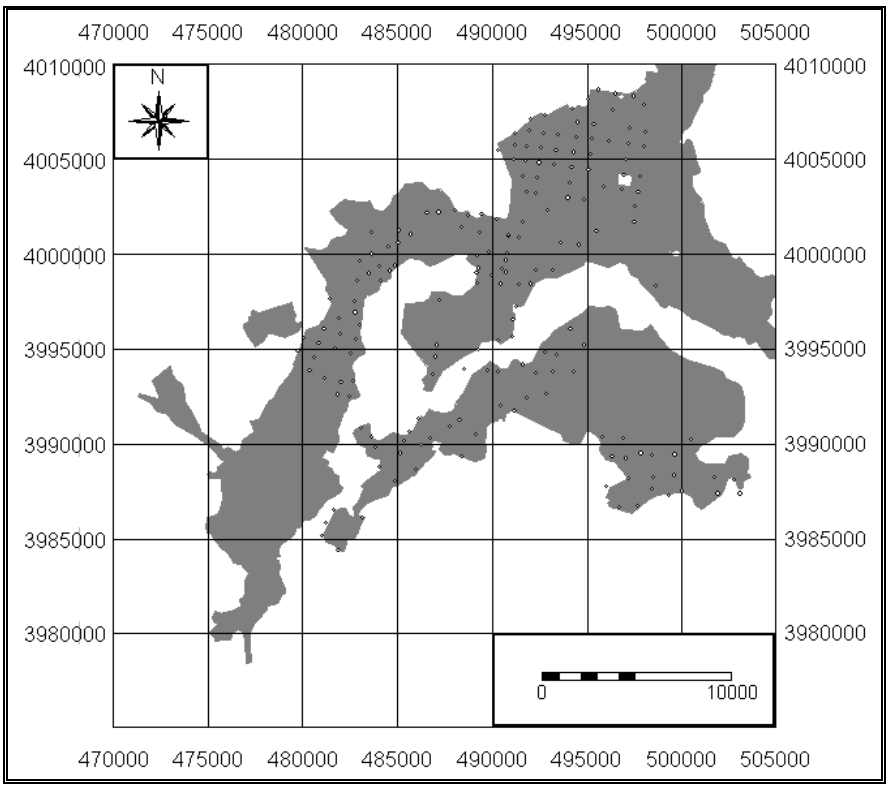

Figure 3.3 Distribution of the existing piezometers in the area.

3.4 Satellite data

3.4.1 General information

In this study two kinds of satellite images have been used Landsat7 and ASTER. Since the 1970's, Landsat satellites have been collecting multispectral images of the Earth's land surface. This unique data archive has played an important role across disciplines as a tool used toward achieving improved understanding of the Earth's land surfaces and human impacts on the environment.

The purpose of the Landsat program is to provide the world's scientists and application engineers with a continuing stream of remote sensing data for monitoring and managing the Earth's resources. Landsat 7 is the latest NASA satellite in a series that has produced an uninterrupted multispectral record of the Earth's land surface since 1972.

The Advanced Space borne Thermal Emission and Reflection Radiometer (ASTER) is an advanced multispectral imager that was launched on board NASA's Terra spacecraft in December 1999. ASTER covers a wide spectral region with 14 bands from the visible to the thermal infrared with high spatial, spectral and radiometric resolution. An additional backward-looking near-infrared band provides stereo coverage.

ASTER consists of three different subsystems: the Visible and Near-infrared (VNIR) has three bands with a spatial resolution of 15 m, and an additional backward telescope for stereo; the Short-wave Infrared (SWIR) has 6 bands with a spatial resolution of 30 m; and the Thermal Infrared (TIR) has 5 bands with a spatial resolution of 90 m. Each subsystem operates in a different spectral region and with its own telescope(s).

Figure 3.4 shows the relation between the wavelengths and wave ranges between landsat7 (ETM) and ASTER.

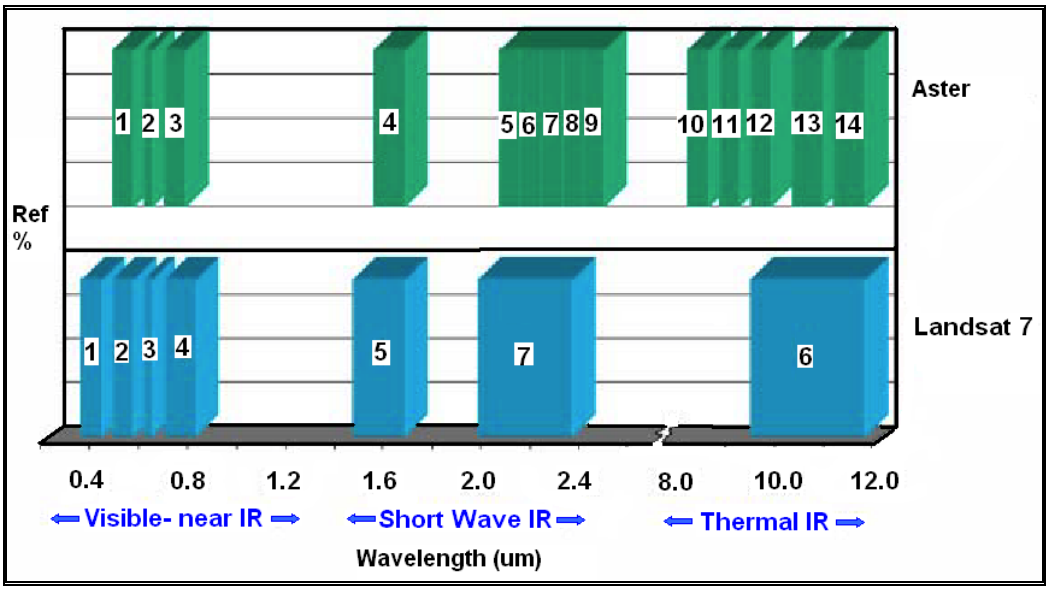

Figure 3.4 Comparison of spectral bands between (ASTER) and (Landsat7 ETM)

Table 3.3 illustrates the spectral bands and the resolution for both kinds of images.

Table 3.3 Landsat versus ASTER

ASTER			Landsat-TM			
	band number	spectral range (μm)	spatial resolution (m)	band number	spectral range (μm)	spatial resolution (m)
VNIR				1	0.45 - 0.52	30
	1	0.52 - 0.60	15	2	0.52 - 0.60	
	2	0.63 - 0.69		3	0.63 - 0.69	
	3	0.76 - 0.86		4	0.76 - 0.90	
SWIR	4	1.60 - 1.70	30	5	1.55 - 1.75	
	5	2.145 - 2.185		7	2.08 - 2.35	
	6	2.185 - 2.225				
	7	2.235 - 2.285				
	8	2.295 - 2.365				
	9	2.360 - 2.430				
TIR	10	8.125 - 8.475	90			
	11	8.475 - 8.825				
	12	8.925 - 9.275				
	13	10.25 - 10.95		6	10.4 - 12.5	60/120 (ETM7/TM5)
	14	10.95 - 11.65				

3.4.2 Landsat 7, ETM path "173" row " 35", date August 24th 2002.

A cloud free image captured during the period of the fieldwork was ordered.

Before using the image in the study, it was necessary to give a coordinate system and geo-reference. The coordinate system (named *balikh*) has UTM projection, WGS 1984 datum, and WGS 84 ellipsoid. The UTM zone is "37", northern hemisphere. Many ground control points were used in creating this coordinate system.

Corners georeference was built on the mentioned coordinate system, with pixel size of 15m.

The image was resampled to this georeference using the nearest point method.

The transforming of the raw data "digital numbers" of the image bands into spectral radiances (w. $m^{-2}.sr^{-1}.\mu m^{-1}$) was done using linear interpolation formula, which, was given within the metadata of the image.

Figure 3.5 shows a pseudo-natural colour composite (RGB for bands (3,4,2)) for the raw Landsat image. Vegetation appears in green because plants have high reflectance in the near

infrared region of the light spectrum, and green colour was assigned for band 4. Figure 3.6 shows the study area after giving the image coordinate system and georeference.

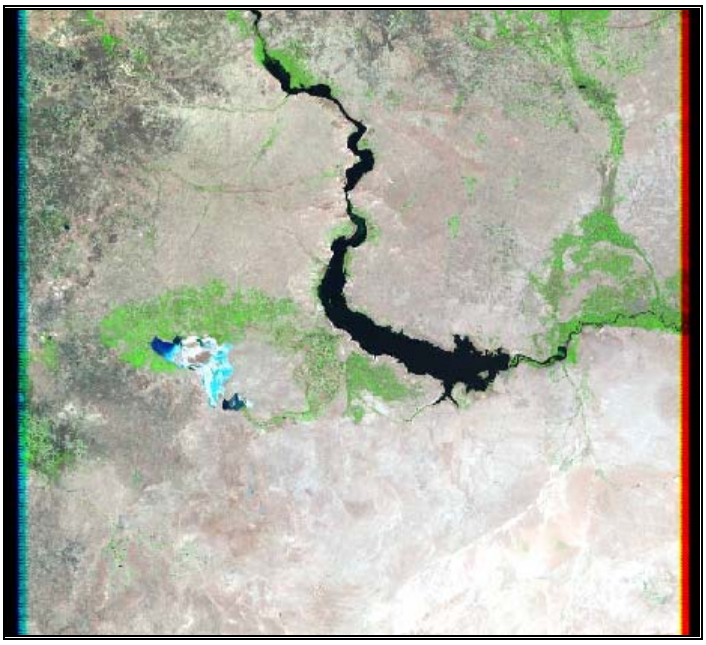

Figure 3.5 Raw Landsat7 image, (FCC), August 24th 2002

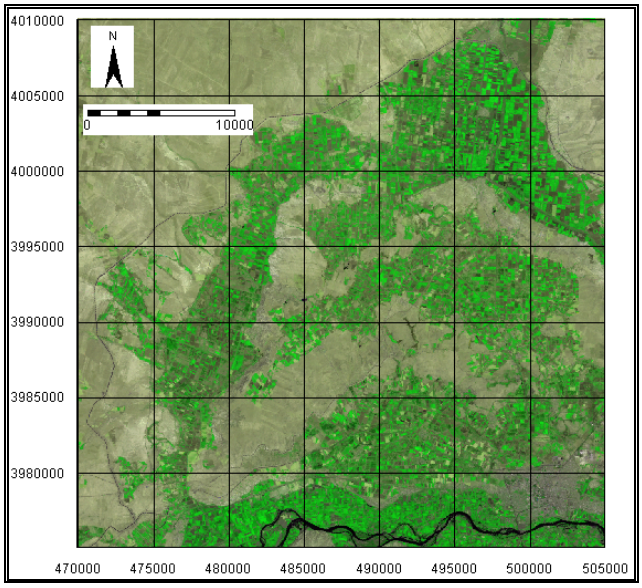

Figure 3.6 Landsat7 after Georeferencing, August 24th 2002

3.4.3 Two sequential ASTER images for the study area March 10th 2002.

These two images were captured sequently in the 10th of March 2002, they are together cover the study area, and they are cloud free.

The same process has been applied to these two images:

They were given the same coordinate system "Balikh", and the same georeference. And then they were glued together to have the same borders "corners" as Landsat image and of course with the same pixel size. Figure 3.7 shows the two raw images in (pseudo-natural colour composite) RGB for bands (2,3,1), also near infrared band (3) displayed in green. Figure 3.8 shows the study area after giving the image coordinate system and georeference.

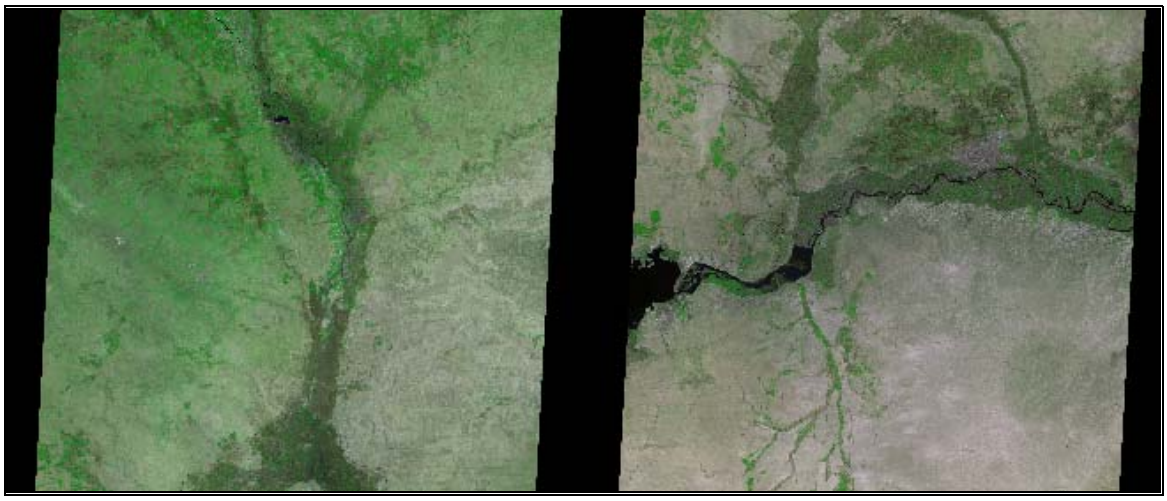

Figure 3.7 Two raw ASTER images, (FCC), March 10th 2002

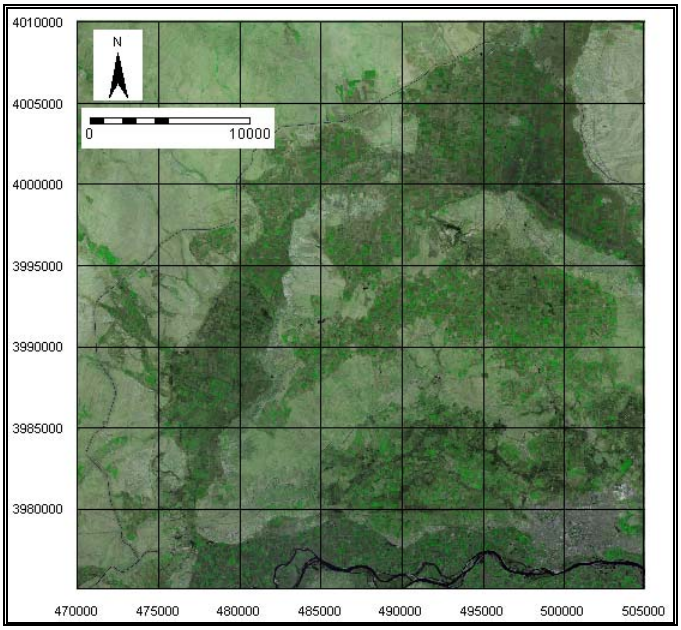

Figure 3.8 Two ASTER images after georeferencing and glueing, March 10th 2002

Chapter 4 Methods

Two methods have been followed to detect salinity in the cotton fields in the area: an empirical and a biophysical one. The empirical method was applied to the ASTER image in March while the biophysical method made use of the Landsat image in August.

4.1 The empirical reflectance method for ASTER

During the field visit, special attention was given to GPS readings and field impression. The selection of the fields is based on "healthy" soil regions and the salt-affected soils. Besides, the wide areas of flourishing salt were identified and also geo-registered with GPS readings.

A work plan for a field survey was designed according to the features noticeable on the ASTER image. The areas of healthy crops and poor crops were determined by the color spectrum of the ASTER image, Pseudo-natural colour composite (RGB for bands (2,3,1)) After the fieldwork had been finished, the range of salinity measurements were identical to those expected according to ASTER image. Therefore, this observation strongly suggests that a relationship between the reflectance of the bare fields in March and the vitality of the growing crops in August exists. The spectral reflectance of saline soils was obtained by plotting the reflectance values (Figure 4.1.).

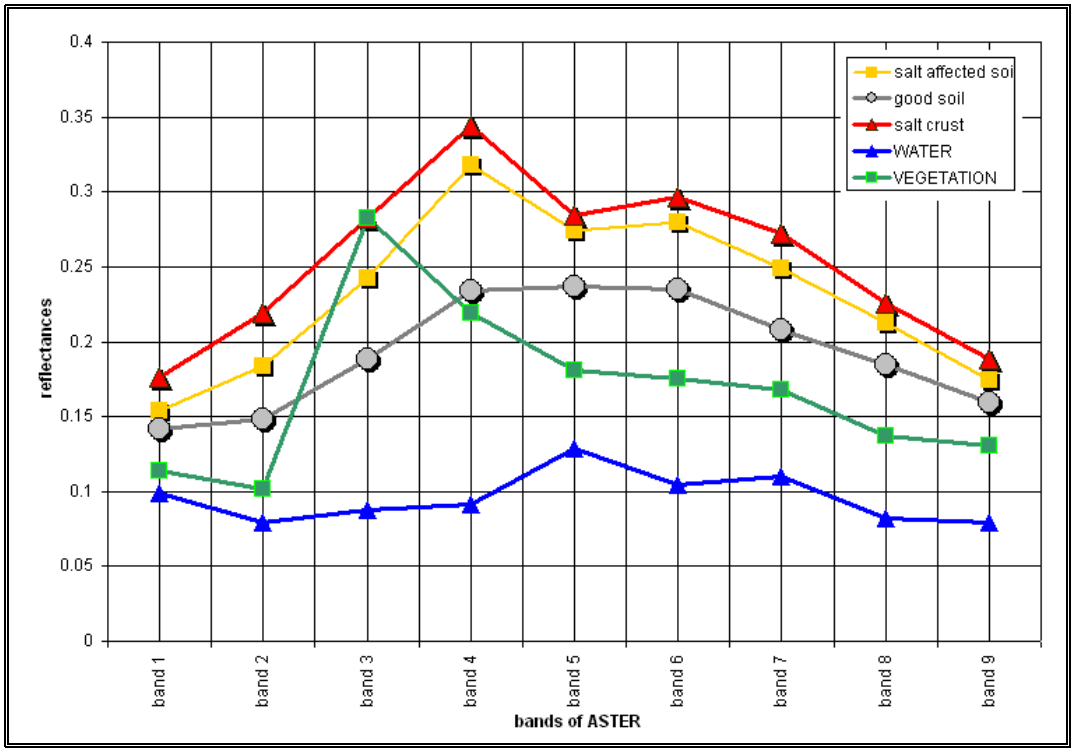

Figure 4.1 Different reflectance for water, vegetation and different salt-continent soils

This simple analysis of Fig. 4.1 shows that there is a relation between the existence of salts in

the soil surface and the difference between bands 4 and 5. Another remark could be taken about this figure that is that more salt in the soil provides a higher reflectance in all bands. This was also concluded in earlier Landsat-based salinity research studies. Menenti et al (1986) found that TM bands 1 through 5 and 7 are good for identifying salt minerals. They plotted the spectral reflectances of different physiographic units in the Kasserine and Saftimi areas in Tunisia with the spectral reflectance of the dominant salt minerals in the two areas. Hovis (1966) gave the reference spectral reflectances of CACO3, CASO4.2 H2O and gypsum sand, as measured in the laboratory. They concluded that salt minerals can be detected when they are a major soil constituent.

Mulders and Epema (1986) used a TM scene as an indicator of gypsum, lime and clay. They graphed some sample units A through G in Saftimi area in Tunisia (see table 4.1 and Figure 4.2)

Table 4.1 Different units in Saftimi area in Tunisia (after Mulders and Epema , 1986)

Land unit		Soil texture	Gypsum crust	Stones	NaCl crust
(A)	glacis	medium	>10	20-50	-
(B)	glacis with sand cover	coarse	>10	20-50	-
(C)	dunes	coarse	<10	<2	-
(K)	Sebkha	coarse	-	-	>20
(H)	Sebkha	fine	-	-	>20
(I)	Chott	coarse	-	-	>20
(G)	oasis				

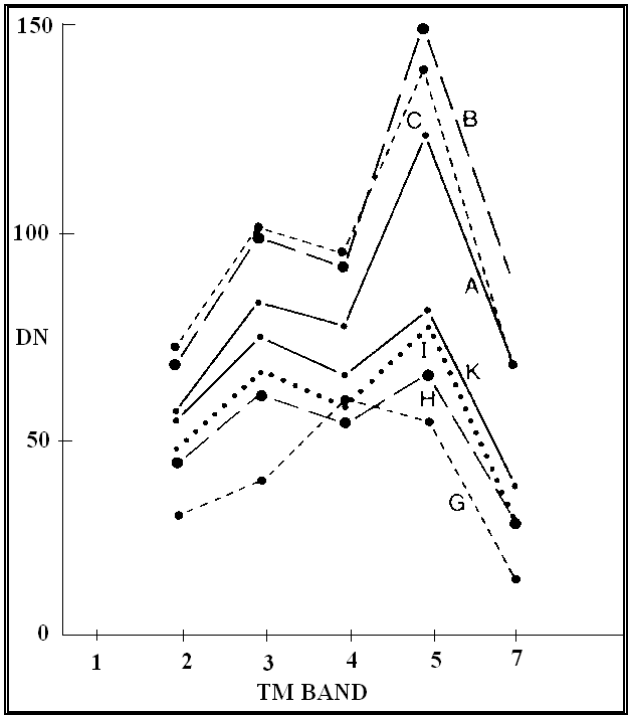

Figure 4.2 Digital numbers of TM bands 2 through 5 and 7 in Tunisia (After Mulders and Epema, 1986)

They discriminated these land units on the basis of a single thematic mapper scene. Especially TM bands (4, 5 and 7) seemed to be suitable.

Also Saha et al. (1990) used the spectral signatures (spectral responses in different bands) with the help of ground data and statistic to differentiate the wasteland categories (salt-affected and waterlogged) and other land use features in India (Figure 4.3). They observed that out of six TM bands (1,2,3,4,5 and 7), four, namely bands 3,4,5 and 7, were poorly correlated, and the spectral separability was greater in bands 4,5 and 7 for all the wasteland categories. This implies that the spectral region between 1.5 and 2.5 μm is suitable to the presence of salts.

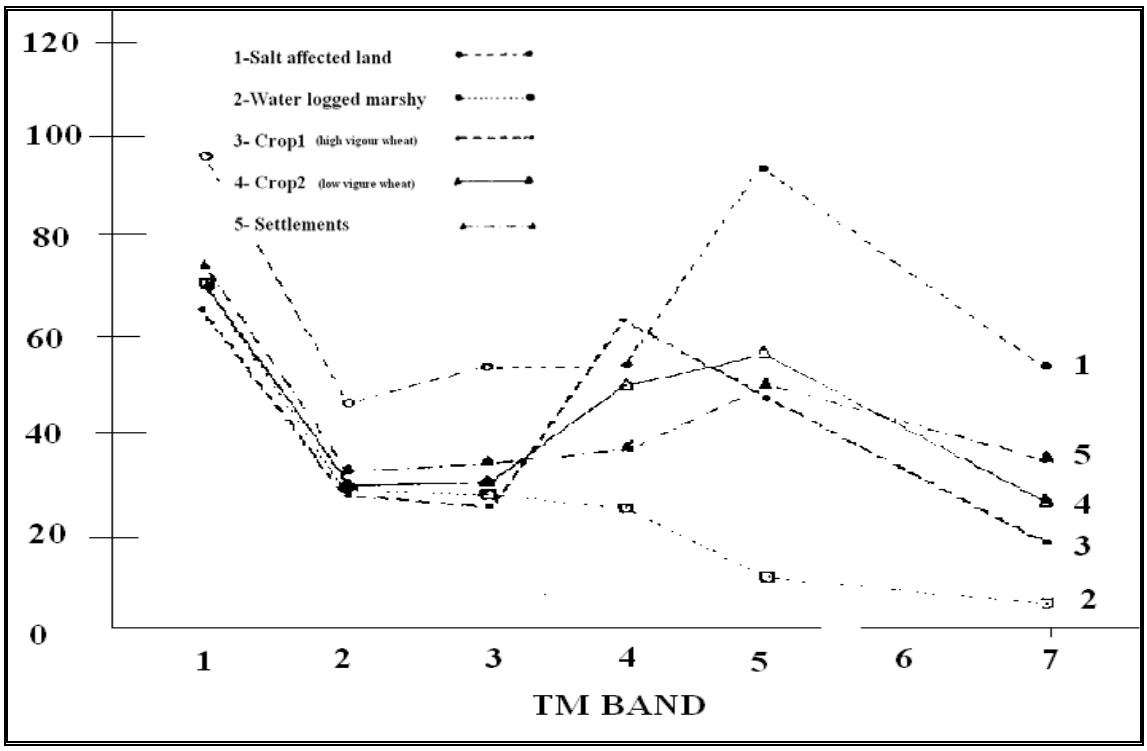

Figure 4.3 Spectral signatures of different wasteland categories and other Landuse features in India (after Saha et al., 1990)

Furthermore, when the ASTER reflectivity are compared with the Landsat bands. The similarity in range between ASTER bands 3, 4 and 5 and bands 4, 5 and 7 from Thematic Mapper is clear. Band 7 of Landsat is, however, spectrally seen much wider and this adversely affects the accuracy to detect soil salinity. Salinity absorption bands have to be small for recognition. The major problem of this reflectance approach is that the cropped surface is a mixture of leaves, soil, salinity and moisture: hence, the measured spectra per definition cannot describe the salinity of the top soil.

It is necessary to emphasis here that the last mentioned bands “4, 5 and 7” were repeatedly used and checked for their potential of detecting saline soils. (Mulders and Epema, 1986; Menenti, Lorkeers and Vissers, 1986; Zuluaga, 1990; Vincent et al.,1996).

Two Indexes From ASTER Bands:

According to the previous analysis two simple reflectance-based indexes were created

1. The ASTER-4, 5 index, produced by ASTER bands $\left(\frac{band4-band5}{band4+band5}\right)$, is according to the data presented of Fig. 4.2 and theoretical aspects, supposed to be a suitable descriptor for overall salinity in the bare agriculture soils. And this hypothesis to be validated later using the available field data.

2. The ASTER-4, 3 index, which is produced by ASTER bands $\left(\frac{band4-band3}{band4+band3}\right)$, has expected detection of the soil composition such as nitrogen or iron dioxides. The latter index is purely produced by experimental work and through trial and error. The results were correlated with "NDVI" obtained from landsat7 in August 24$^{th.}$

The validation for both indexes was conducted using NDVI in August, assuming that a larger NDVI expresses successful crop growth, and less harmful salts in the soils.

4.2 The biophysical method for Landsat 7 (ETM):

4.2.1 Theoretical background:

This method is built on the concept of surface resistance. This resistance describes the vapor flow through the transpiring crop and evaporating soil when the soil is not completely covered by canopies (Figure 4.4).

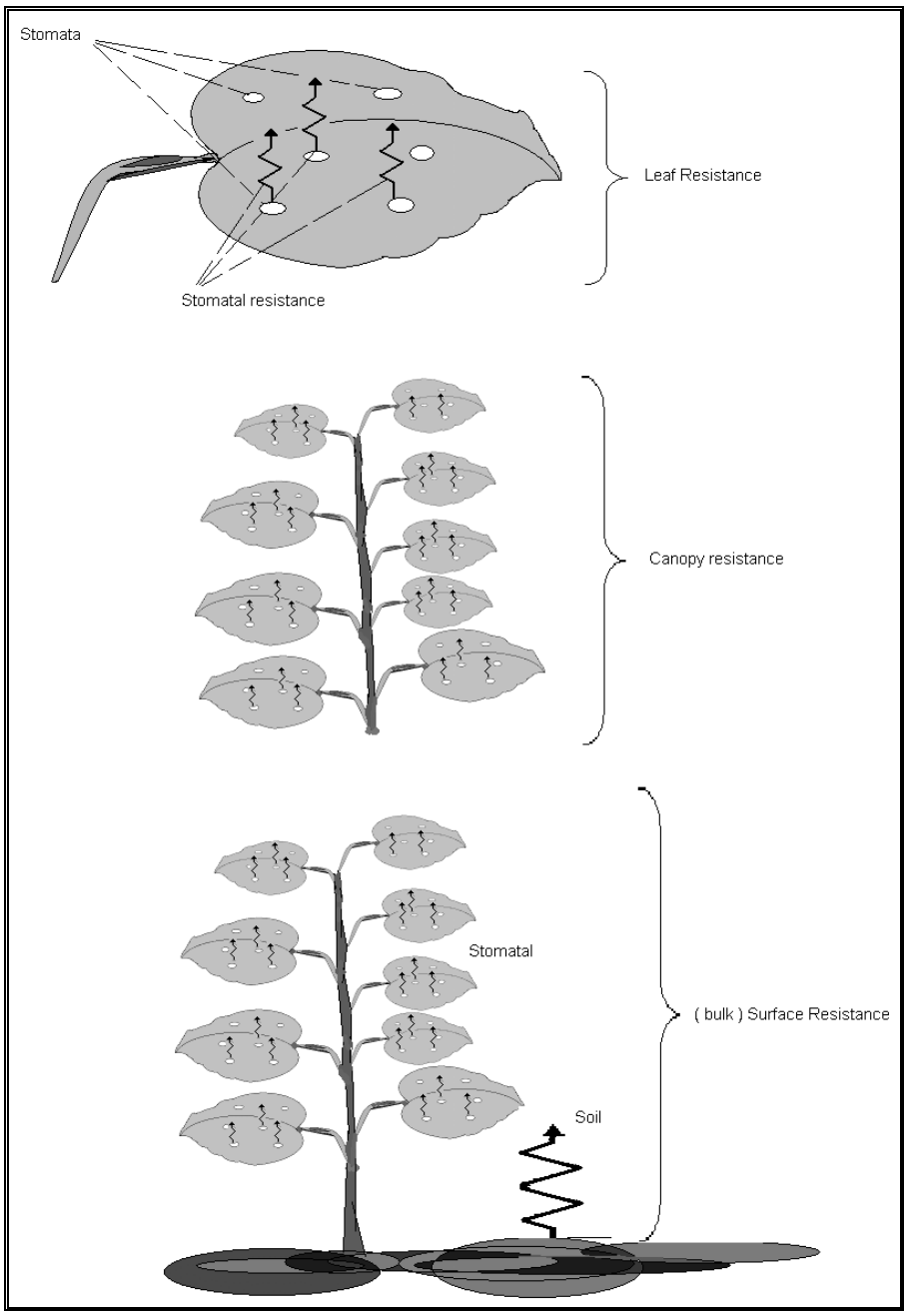

Figure 4.4 Surface resistance for the plants.

The surface resistance, r_s, represents the effect of soil moisture and solute concentration on actual evapotransperation.

The bulk stomatal resistance, r_l, is the average resistance of an individual leaf. This resistance is crop specific and differs among crop varieties and crop management. It is usually increased as the crop ages and begins to ripen. The information available in the literature on stomatal conductance is often oriented toward physiological or ecophysiological studies, and not often to the state conditions of the soil column.

4.2.2 The relation between the surface resistance and soil salinity,

The adverse effects of salts on plants are generally divided into two categories. The first and most important one is the total salt or osmotic effect on the ability of the plant to take up water from the soil solution. Crop growth reduction due to salinity is generally related to the soil solution osmotic potential of the root zone. All soluble salts contribute to the osmotic effect. When salt is dissolved in water, the potential energy of water is lowered and the plant must spend more energy to take up water from the same soil water content.

The second category consists of specific ion effects, because an excess of specific ions maybe toxic to various plant physiological processes (Homaee, 1999). The predominant influence of salinity stress on plants is suppression of root water uptake and growth. This suppression is typically a nonspecific salt effect, depending more on osmotic stress created by total concentration of soluble salts than on the level of specific solutes (Homaee, 1999).

The quantitive response of plants to salinity stress is usually described through the yield response to electrical conductivity of the soil solution ECe. Brown and Hayward (1956), Lunin et al. (1963), Shalhevet et al. (1969), and Mass and Hoffman (1977) suggested that the reduction in crop yield due to salinity could be linearly related to the electrical conductivity of the soil solution.

The response function of Maas and Hoffman can be written as:

$$\frac{Y_{act}}{Y_{pot}} = 1 . \qquad \text{For } 0 \leq EC_e \leq EC_e^* \qquad (4.1)$$

$$\frac{Y_{act}}{Y_{pot}} = 100 - \alpha(EC_e - EC_e^*) . \qquad \text{For } EC_e > EC_e^* \qquad (4.2)$$

Where EC_e ($dS.m^{-1}$) is the electrical conductivity of the soil saturation extract; EC_e^* ($dS.m^{-1}$) is the threshold value of salinity at which relative begins to decrease; and α (m/dS) is the slope which indicates the present yield decrease per unit salinity increase (Figure 4.5). This equation is valid when EC_e is higher than the threshold value and less than the value resulting in zero yield.

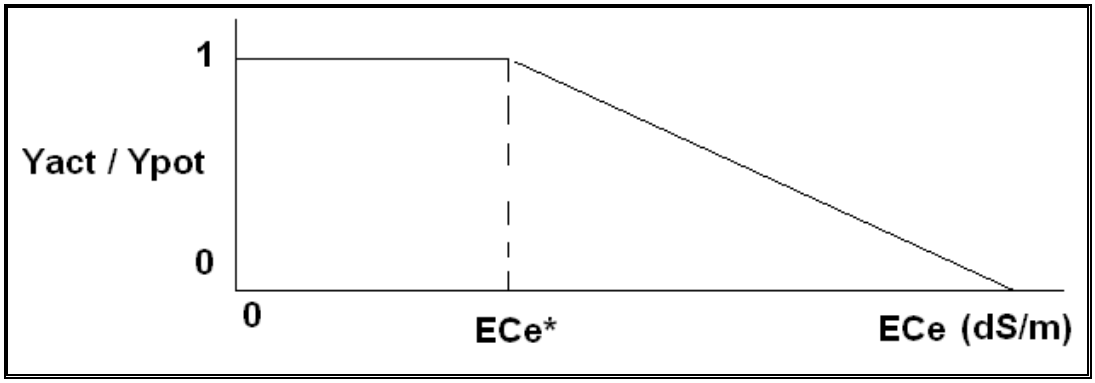

Figure 4.5 Relative yield $\left(\frac{Y_{act}}{Y_{pot}}\right)$ versus the electrical conductivity of the soil extract EC_e.

Assuming that relative yield (Y_{act} / Y_{pot}) has a one to one relationship with relative transpiration (T_{act}/T_{pot}) and thus with relative root water uptake over the entire root zone, we can write that under saline conditions:

$$\frac{Y_{act}}{Y_{pot}} = \frac{T_{act}}{T_{pot}} = f(EC_e) = \alpha_{rs}(\pi)\,. \qquad (4.3)$$

Where π (cm) is the osmotic pressure head. To convert the electrical conductivity based slope α into an osmotic head based slope (figure 4.6), one may use a factor of 360 (Richards, 1954): π=-360 *EC_e. Hence

$\alpha_{rs}(\pi)$ =1. For $0 \leq \pi \leq \pi^*$ (4.4)

$$\alpha_{rs}(\pi) = 1 - \frac{\alpha}{360}(\pi - \pi^*)\,. \qquad \text{For } \pi > \pi^* \qquad (4.5)$$

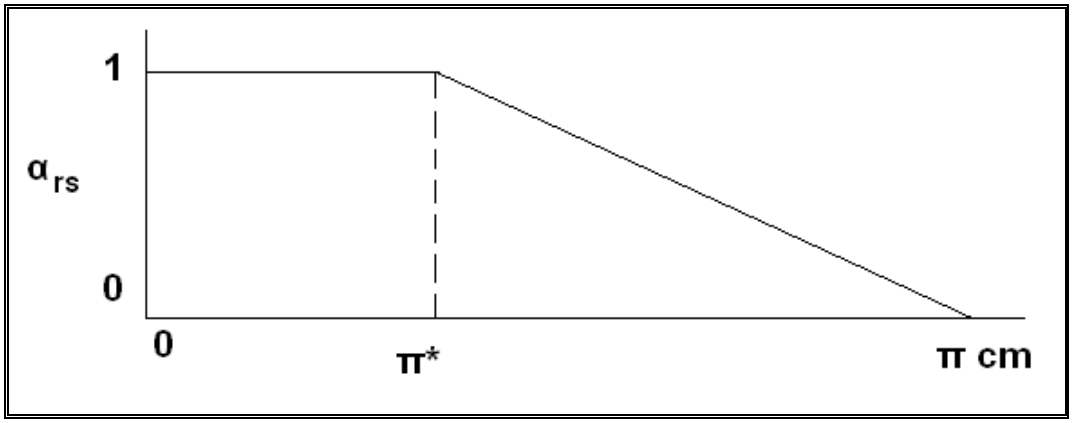

Figure 4.6 Root water uptake reduction function α_{rs} versus osmotic head π.

The relation between the soil water pressure head π and EC_e is linear. The biophysical meaning of α can be explained by the surface resistance r_s. Jarvis (1976) and later Hanan and Prince (1997) developed a model that estimates r_s as:

$$r_s = \frac{r_{s\min}}{LAI \quad F_1(T_a)F_2(\Delta e)F_3(h_{rw})} \tag{4.6}$$

The function $F_1(T_\alpha)$ represents the thermal stress on stomatal closure due to the effect of air temperature T_α on r_s. The function F2 (Δ_e) represents the effect of the vapour pressure deficit on the opening of stomata, and the function F3 (h_{rw}) is represents the effect of the soil water pressure head. $F_3(h_{rw})$ can be further worked out as:

$$F_3(h_{rw}) = 1 - \frac{h_{\max} - h_{rw}}{h_{\max} - c} \tag{4.7}$$

Where h_{rw} (cm) is the average root-weighted soil water pressure head, c is the soil water pressure head at which stress is due to soil water pressure head is triggered and h_{max} is the soil water pressure head at which wilting occurs.

From this equation, it is obvious that the relation between the osmotic pressure head and the surface resistance is inversely proportional and then The physical coupling between salinity and surface resistance is herewith explained.

The surface resistance was calculated for the study area from the Landsat image using Penman Monteith equation along with SEBAL algorithm (Surface Energy Balance Algorithm For Land):

$$\lambda E = \frac{s_a(R_n - G_0) + \rho_a c_p \Delta e / r_a}{s_a + \gamma(1 + r_s/r_a)} \ (\mathrm{Wm^{-2}}) \tag{4.8}$$

Where λE is the actual evaporation determined by SEBAL, s_a (mbar K^{-1}) is the slope of the saturated vapor pressure curve, ρ_a (kg m^{-3}) is the moist air density, c_p (J kg^{-1} K^{-1}) is the air specific heat at constant pressure, Δe (mbar) is the air vapor deficit from saturation, r_a (s m^{-1}) is the aerodynamic resistance and r_s (s m^{-1}) is the surface resistance. Since r_s is the only unknown, it can be solved from the inversion of the Penman-Monteith equation (see Farah, 2000). The parameters of this equation can be calculated as following.

1. s_a is a function of air temperature T. (^oC)

$$s_a = 4098 \cdot \frac{0.6108 \cdot e^{\left[\frac{17.27T}{T+237.3}\right]}}{(T+237.3)^2} \tag{4.9}$$

2. $\Delta e = e_s - e_a$

e_s is a function of air temperature

e_a is a function of dew point temperature

3. G_0 = 0 for 24 hours.
4. γ = 0.0643 psychrometric constant
5. R_n , ΔT, H and λE are maps and are obtained from SEBAL algorithm.

4.2.3 SEBAL algorithm, Surface Energy Balance Algorithm For Land, a brief description:

The energy received from the sun is the main source that governs the heat and water exchange processes in the soil plant and atmosphere system. The energy fluxes are combined in a surface energy balance that describes the partitioning of the available energy as:

$$R_n = G_o + H + LE \quad (4.10)$$

Where R_n is the net radiation flux density (Wm^{-2}), G_o soil heat flux density (Wm^{-2}), H is sensible heat flux density (Wm^{-2}) and LE is latent heat flux density (Wm^{-2}).

Net Radiation, R_n:

The net radiation is the resultant of all incoming and outgoing radiation:

$$R_n = K_{in} - K_{out} + L_{in} - L_{out} \ (Wm^{-2}) \quad (4.11)$$

Where K_{in} and K_{out} (Wm^{-2}) are the incoming and outgoing short-wave radiations respectively. And L_{in} and L_{out} (Wm^{-2}) are the incoming and outgoing long wave radiations respectively. The amount of incoming short wave radiation, K_{in} is a function of time and place of that particular place on the earth. K_{out} is the radiation reflected by the earth surface. The ratio between K_{in} and K_{out} is called as surface albedo (r_o) and therefore, the net short-wave radiation can be written as (1- r_o) K_{in}.

The incoming long wave radiation, L_{in} is the radiation emitted by the atmosphere described by the law of Stefan-Boltzmann. As expressed below:

$$L_{in} = \varepsilon * \sigma * T_a^4 \quad (4.12)$$

where: ε is the apparent atmospheric emissivity, σ is Stefan-Boltzmann constant (W m^{-2} K^{-4}), and T_a is the atmospheric temperature (K). The energy emitted from the earth surface can be described as:

$$L_{out} = \varepsilon_o * \sigma * T_o^4 \quad (4.13)$$

where: ε_o is the grey body emissivity, σ is Stefan-Boltzmann constant (W m^{-2} K^{-4}), and T_o is the surface temperature (k).

Soil heat flux, G_o:

The soil heat flux is the energy used for warming or cooling the subsurface soil volume. It is determined by the thermal conductivity of the soil and the temperature gradient of the top soil.

$$G_o = R_n \cdot \left\{ \frac{(T_o - 273)}{r_o} \cdot \left[0.00332 \cdot (c_1 \cdot r_o) + 0.0062 \cdot (c_1 \cdot r_o)^2 \right] \cdot (1 - 0.978 \cdot NDVI^4) \right\} \quad (4.14)$$

where:
R_n is the instantaneous net radiation map in watt/m^2
T_o is the surface temperature map in Kelvin
r_o is the surface broadband albedo map (non-dimensional)
NDVI is the normalized vegetation index (non-dimensional)
C_1 is a factor to convert the instantaneous values of albedo to daily averages (default = 1.1)

Sensible heat flux, H:

The sensible heat flux is the heat transfer between the ground and the temperature, enhanced by forced or free convection.

$$H = (\rho_a C_p / r_{ah}) * \delta T_{a\text{-}sur} \quad (4.15)$$

Where $\rho_a C_p$ is air heat capacity (J m^3 K^{-1}), r_{ah} is the aerodynamic resistance to heat transfer (s m^{-1}) and $\delta T_{a\text{-}sur}$ is air to surface difference (K).

Latent heat flux, LE:

The latent heat flux describes the energy used for evaporation of moisture from land surface element. Since, all the components of surface energy balance are solved, latent heat flux can be determined as residual of the surface energy balance equation.

Chapter 5 Results

5.1 Masking out the cotton fields

Because every single crop has its own specific characteristics like the amount of reflectance and the range of the surface resistance it is necessary to distinguish cotton from other crops. So if we want to interpret biophysical parameters, we have to mask out the crop that we focus on.

Cotton is the major summer crop. More than 80% of the summer crops is cotton and that is why all attention is focused on the cotton fields.

The procedures of masking out cotton fields

The process of classifying cotton was easy and straightforward, because its growing stage is different from other possible existing crops like maize or some vegetables during August. The different growing stages have resulted in different reflectance characteristics.

The vegetated area was first masked out in August image using NDVI (Normalized Difference Vegetation Index). An unsupervised classification procedure (with four classes) was thereafter applied to all pixels with a vegetation cover.

From the cropping calendar, it is known that cotton fields are fallow during March. The bare fields in March 10th were masked out (also using NDVI) from the ASTER image and then crossed with the mask obtained from Landsat. The resulting mask map was tested against the field GPS points and the result was accepted because all cotton fields were classified as cotton (Figure 5.1).

5.2 The results of the empirical method

As mentioned in the previous chapter starting from the remark that the good cotton fields locations were anticipated successfully beforehand using the ASTER image, which has been captured while the fields were still bare (March 10^{th} 2002).

Building on that and on the analysis of the reflectance curves of salt affected and healthy soil, together with the aid of the previous work in detecting salinity using Landsat bands which has been reviewed through out the literature, two combination of bands have been tested.

The verification has been conducted using the resulting NDVI in August assuming that a larger NDVI expresses more successful crop growth, and less harmful salts in the soils.

After calculating the index map, the raster map was divided into five* classes, depending on its histogram, with equal number of pixels, with five ranges of that specific index (from the lowest to the highest). At the same time the NDVI map of cotton field in August was divided into five classes also with the same number of pixels and with increasing range of NDVI.

The two maps then were crossed with each other. By this we can observe in each class of the obtained index how much pixels of high NDVI has grown on it, And also how much pixels of medium and low NDVI.

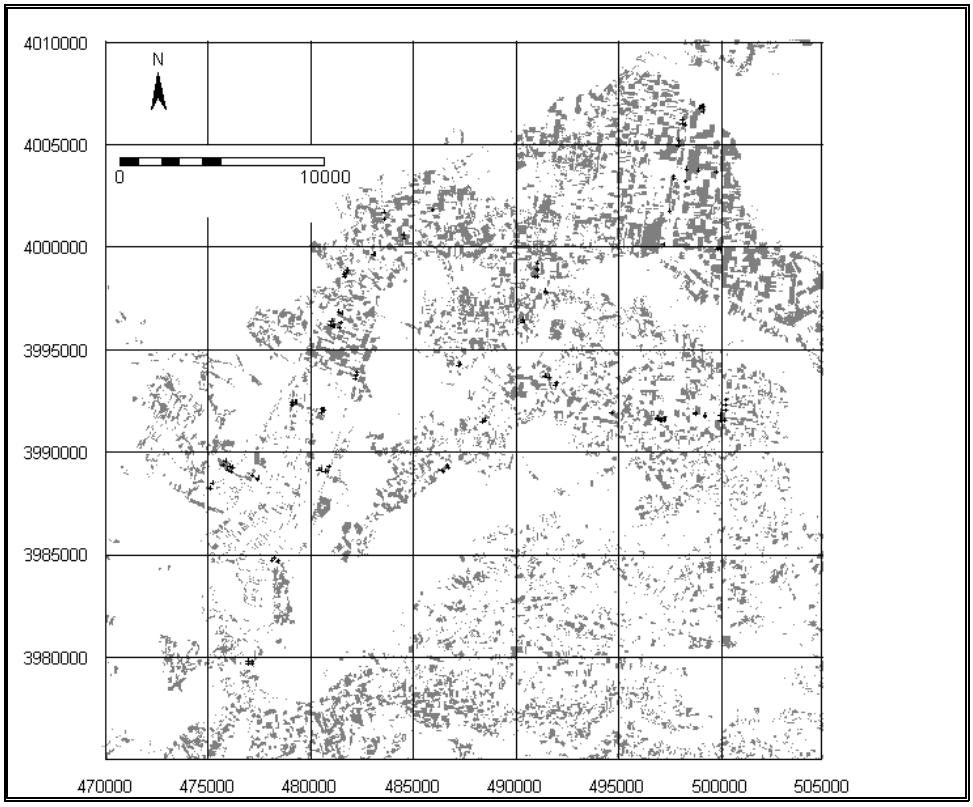

Figure 5.1 Cotton fields map with the GPS Landcover points

The indexes, which were tested, were given identification numbers as follows,

$$\text{Index1}=\left(\frac{band4-band3}{band4+band3}\right)$$

$$\text{Index2}=\left(\frac{band4-band5}{band4+band5}\right)$$

Index1 (figure 5.2) showed that in the middle range of it, the number of the good NDVI (green) is increasing while it is decreasing at the two edges (to the right and to the left). This means that when this index has specific value between (0.077 and 1.077) the NDVI values of the cotton on that land go up, in another meaning cotton is flourishing in August on the land

*In order to simplify the presentation of the result it was useful to use five classes, but in the beginning of the analysis ten classes were used and the analysis gave the same results as five classes.

that has a value of this index between (0.077 and 1.077) in March (when it was fallow). What does support this is that within the mentioned rang the number of pixels of low NDVI values decreases (red bars in figure 5.2).

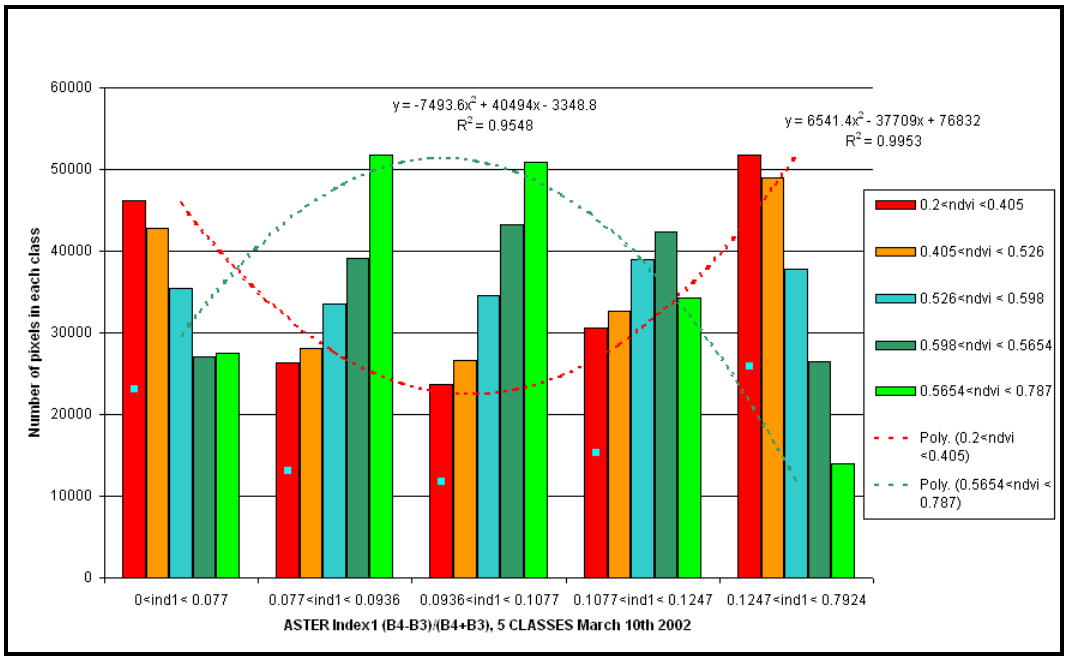

Figure 5.2 The crossing between index1 in March and NDVI in August 2002

The result of this index as shown in figure 5.2 can be interpreted by that this index is detecting a substance, which is necessary to the crop growing success but in certain amount which if increase or decrease it will have bad effects on the success of the crop. This material maybe iron dioxides or nitrogen and this issue need to be more investigated.

The crossing of the second index "**index2"** in March with NDVI in August is shown in figure 5.3. The same as in figure 5.2;the red bars present the number of pixels that have the lowest NDVI value (less than 0.405). Meanwhile the green bars present the number of pixels that have the highest NDVI values, more than 0.5654.

The height of reddish bars is increasing from left to right with the increasing of the index2 values. That means the higher the value of index2 of the fallow land in March the less NDVI values of cotton will grow on that land in August.

At the other hand the height of the green bars is decreasing from left to right with the increasing of index2. In other words the lower the value of index2 of a fallow land in March the higher values of NDVI of cotton will result on it in August.

This can be interpreted by that this index detects a material in the soil. This material is harmful for the plants so the less the better and this most likely will be a kind of salts.

The effect of that material on the success of the cotton in August is illustrated more in figure 5.4. This figure shows the average NDVI values for all pixels, which grow on each class of in-

dex2. The result is that with the increase of index2 values, the average NDVI values in August will decrease linearly.

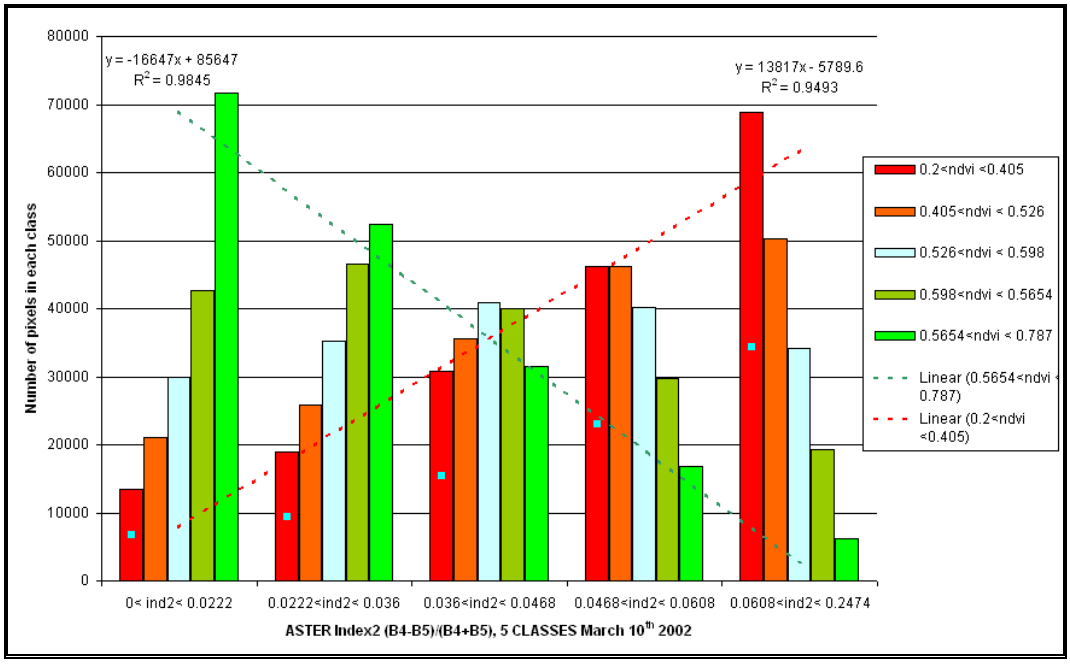

Figure 5.3 The crossing between index2 in March 10th and NDVI in August 24th 2002

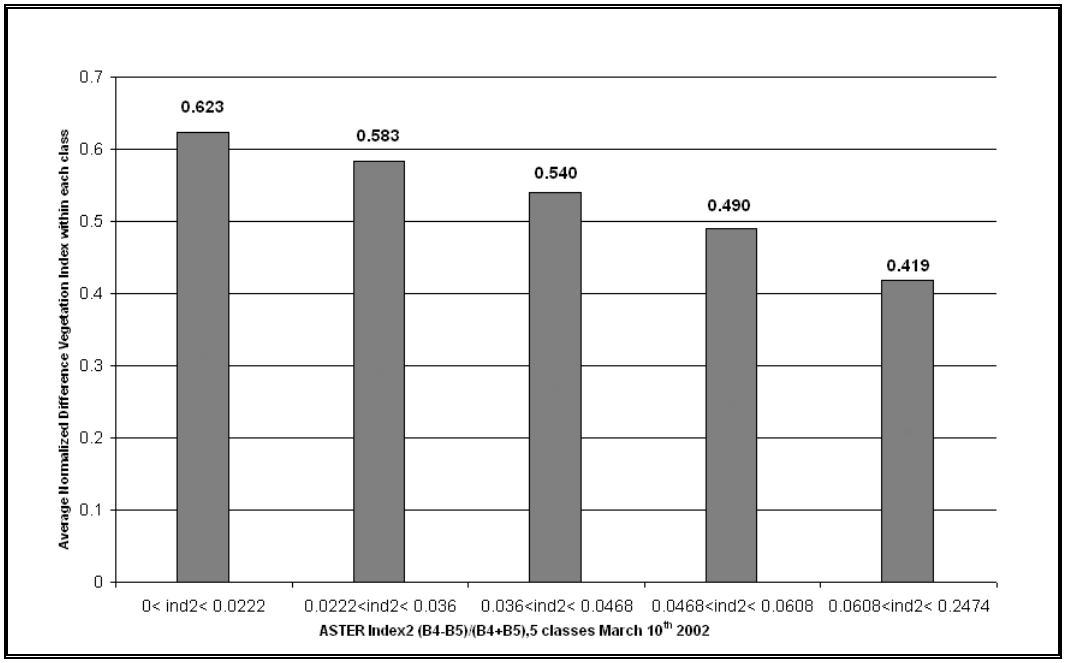

Figure 5.4 Average NDVI in August within each class of index2

This index has also checked with the field data in September (Figure 5.5). The mean ECe values for the fieldwork points were crossed with this index. Figure 5.5 shows that there is a correlation in spite of the long time difference (around six months, from March until September). Keeping in mind that the dynamic nature of the salts in the irrigated fields, as salts are moving in both directions vertically and horizontally, has resulted in the occurrence of many outliers in the Figure, but still the relation does clearly exist.

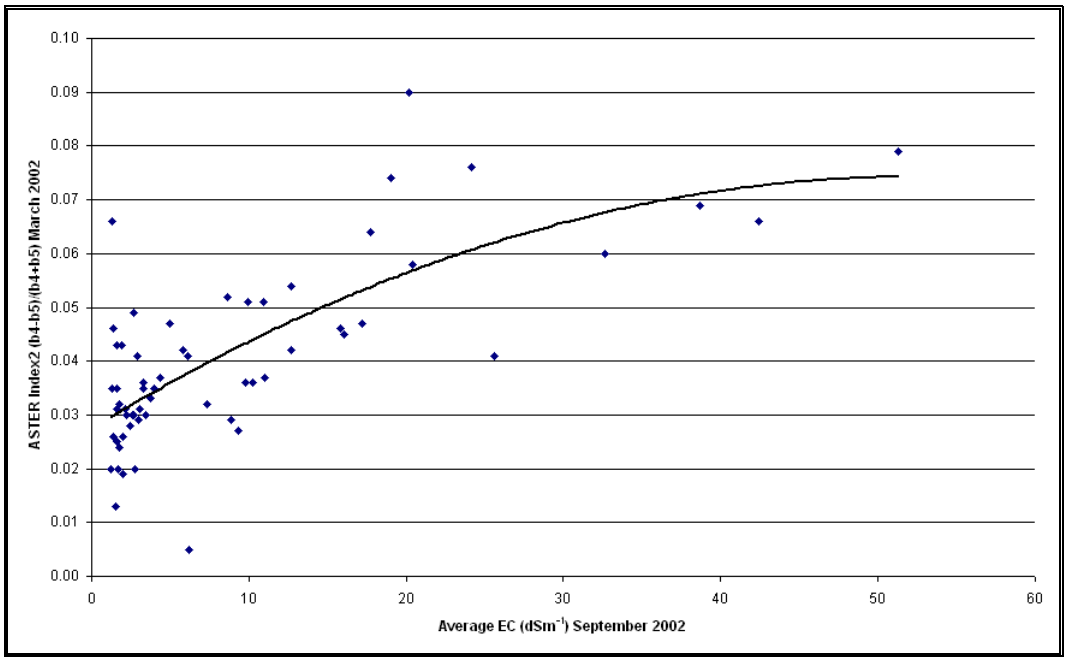

Figure 5.5 Crossing between mean ECe in September and index2 in March

Figure 5.6 shows this index map with five classes. It is clear that the areas of low values of index2 less than 0.0222 occur near the rivers in the south and in upper right. These areas are being cultivated since long time ago. They were irrigated by water from the river and drained into the river in natural way, and they still in good condition and the crops flourishing in them. On the other hand the newly irrigated area (the rest of the map) has ranging values from 0.036 until 0.2474. Some of them are good but not as good as those close to the river and some of them because of the bad functioning drainage, indicate rather poor conditions.

Depending on figure 5.5, figure 5.6 can be interpreted as follows,
When Index2 is less than 0.0222 ➔ EC less than 2 $dS.m^{-1}$ ("clean" soils)
When Index2 is more than 0.0222 and less than 0.036➔ EC more than 2 $dS.m^{-1}$and less than 7 $dS.m^{-1}$
When Index2 is more than 0.036 and less than 0.0468➔ EC more than 7 $dS.m^{-1}$and less than 13 $dS.m^{-1}$
When Index2 is more than 0.0468 and less than 0.0608➔ EC more than 13 $dS.m^{-1}$ and less than 24 $dS.m^{-1}$
When Index2 is more than 0. 0608➔ EC more than 24 $dS.m^{-1}$ (very saline soils)

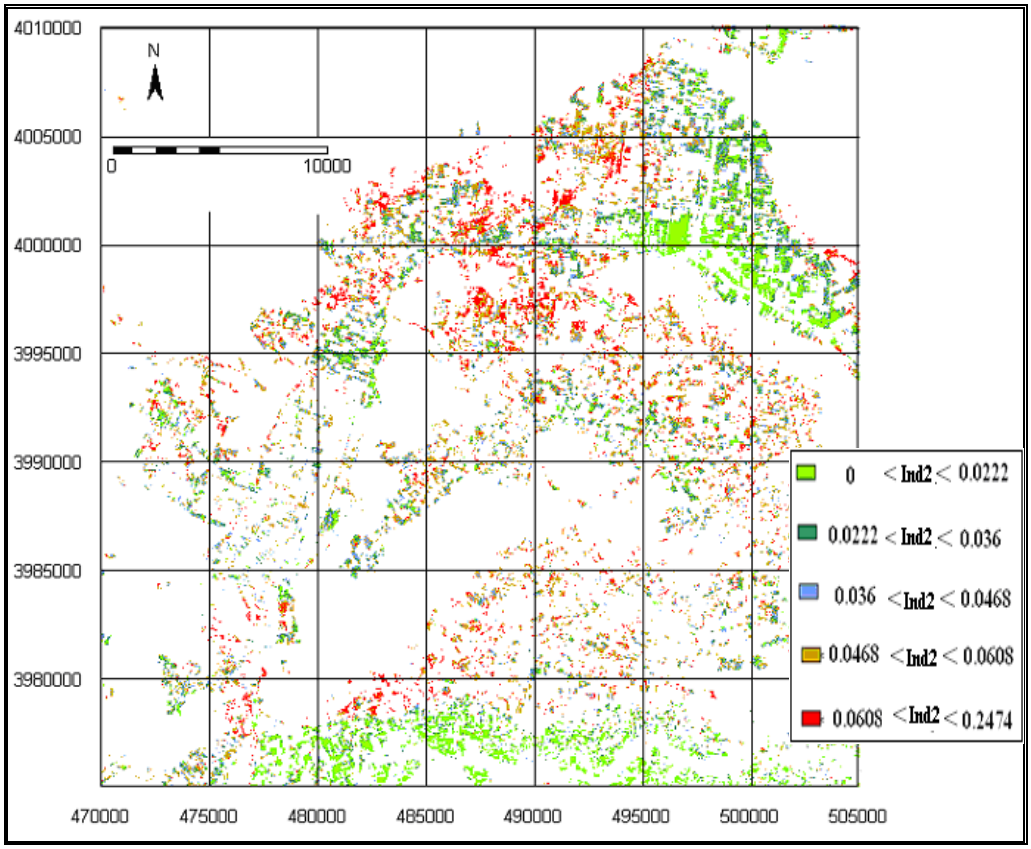

Figure 5.6 Index2 map March 10th 2002, 5 classes

5.3 The results of biophysical method for Landsat 7 ETM

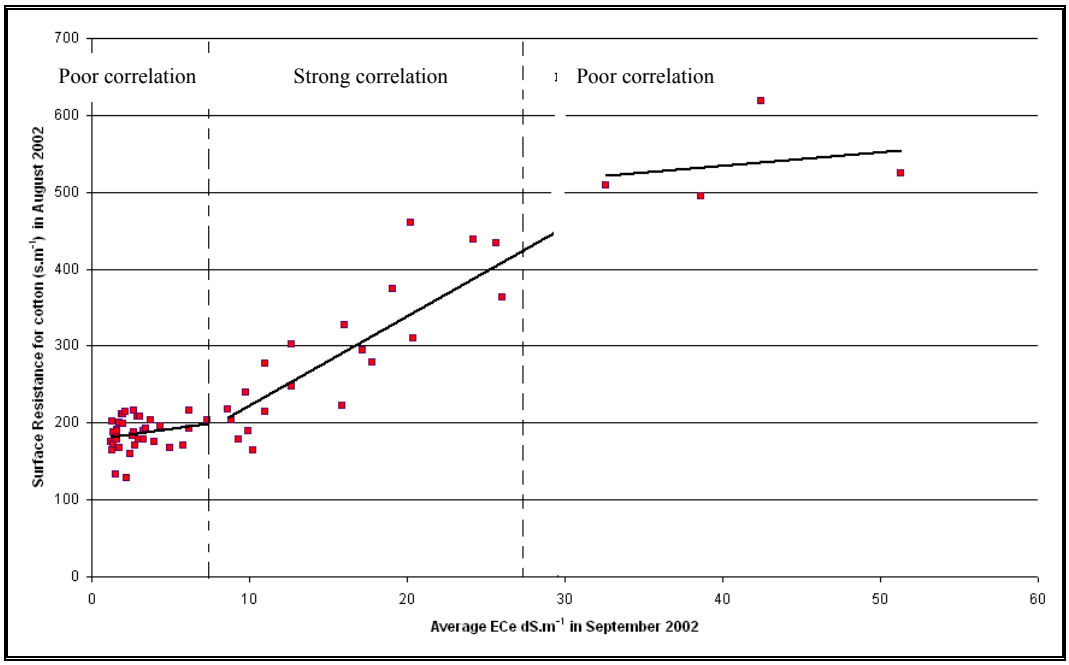

Figure 5.7 Crossing between mean ECe in September and surface resistance in August

After calculating the surface resistance map of the cotton, as described in chapter four, the field data were crossed with the map. Figure 5.7 explains the result of this method.

In fact the result agrees with the well-known response of cotton with salinity stress.

When the mean salinity of the soil is less than 7.7 $dS.m^{-1}$ the crop has no response and no stress. The figure shows that when EC less than 7.7 $dS.m^{-1}$. less correlation between r_s and EC_e. Within this range the crop is flourishing successfully. Figure 5.8 shows two example photos for this state.

Between the values 7.7 and 27 there is an increase of the surface resistance of the crop with the increasing of the mean EC in the soil. So the bigger value for ECe, (the more salinity), the more difficult for the crop to obtain water from the soil, and thus more surface resistance. In fact within this region the correlation between the soil salinity and the surface resistance of the crop is clear. Example photos of this state are shown in figure 5.9.

Then after 27 EC the crop cannot stand the salinity, so again a decreasing correlation is observed between the surface resistance and EC, as shown in figure 5.10

Figure 5.7 is in agreement with Table 1.2 showing the salinity tolerance of cotton.

Figure 5.8 Healthy cotton fields with ECe less than 7.7 dS.m^{-1}

Figure 5.9 Cotton fields with ECe more than 7.7 dS.m^{-1} and less than 27 dS.m^{-1}

Figure 5.10 Cotton fields with ECe more than 27 dS.m^{-1}

Figure 5.11 shows a map of surface resistance for cotton with five classes.

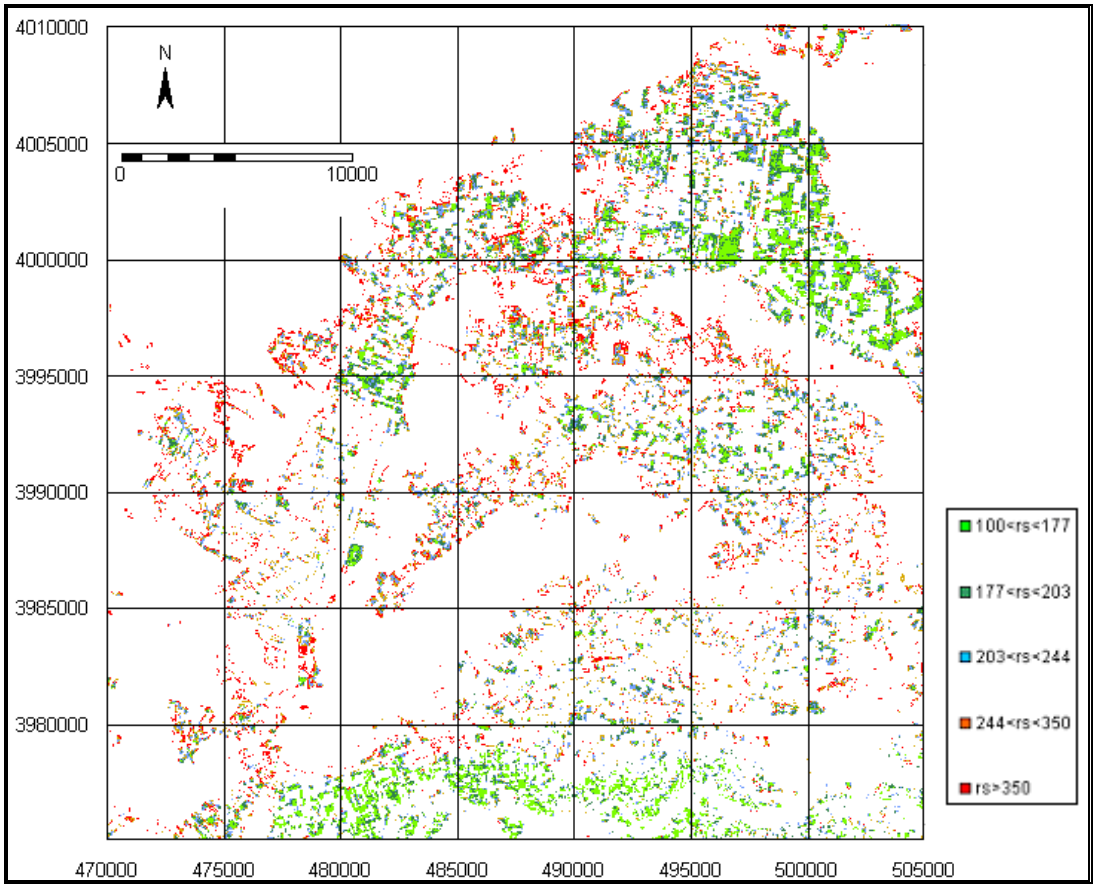

Figure 5.11 Surface resistance (S.m^{-1}) for cotton fields with five classes (August 24th 2002)

Salinity in this area with its specific characteristic has a major effect on the surface resistance more than the other factors like soil water content, or vapour pressure deficit and that because of various reasons. The area is overly supplied with irrigation water and as a result it has become water logged and because of that fields are salt-affected. Figure 5.12 shows the water table depth in the area, which has been interpolated depending on the available readings of the water table depth in July. And it is obvious from that figure that these levels give cause for concern. The soil water content, which obtained throughout the fieldwork, has been crossed with surface resistance (Figure 5.13). The results have shown that the major factor that affects the surface resistance of cotton in this area is soil salinity.

Depending on figure 5.7, figure 5.11can be interpreted as follows,

When r_s is less than 200 S.m^{-1}. ➔ EC less than 7.7 dS.m^{-1}

When r_s is more than 200 S.m^{-1} and less than 250 S.m^{-1}➔ EC more than 7.7 dS.m^{-1} and less than 13 dS.m^{-1}

When r_s is more than 250 S.m^{-1} and less than 350 S.m^{-1} ➔ EC more than 13 dS.m^{-1} and less than 24 dS.m^{-1}

When r_s is more than 350 S.m^{-1} ➔ EC more than 24 dS.m^{-1}

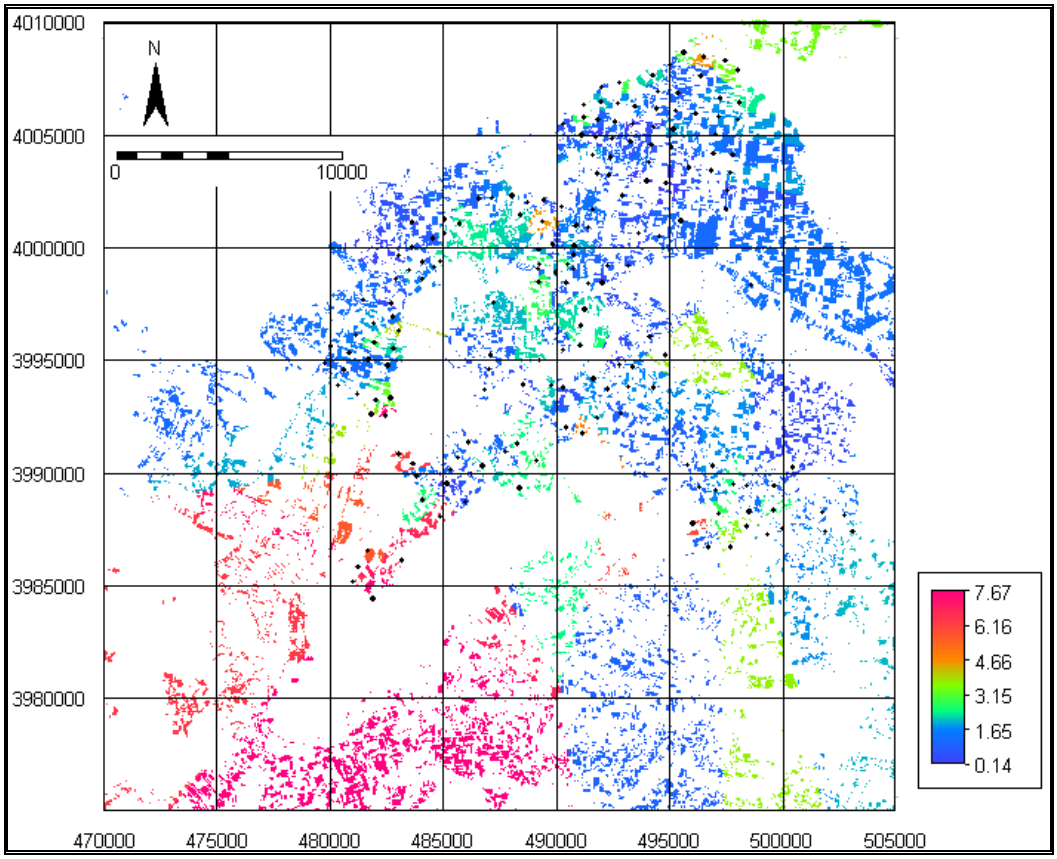

Figure 5.12 The water table depth (m) in July 2002 with the location of the piezometers

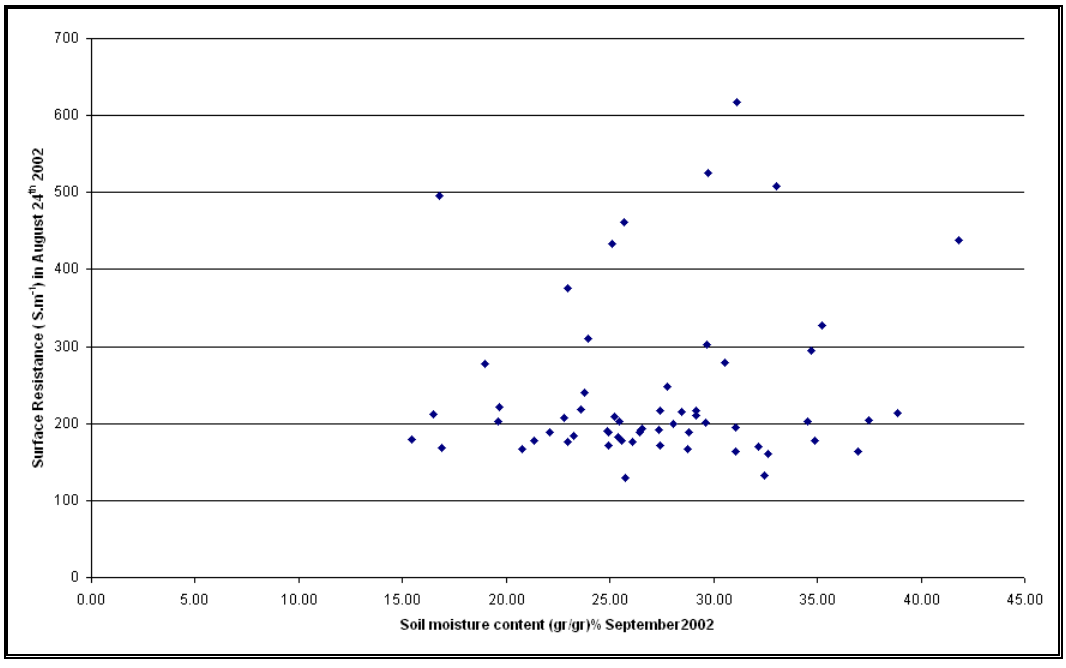

Figure 5.13 Soil water content September 2002 VS surface resistance of cotton August 24th

5.4 Inter seasonal relationship

Finally the results of the two methods were crossed. Figure 5.14 shows that the average surface resistance within each class of index2 is increasing from right to left. When compared between this figure and figure 5.4 the trend here is stronger. So the correlation between the two methods is high.

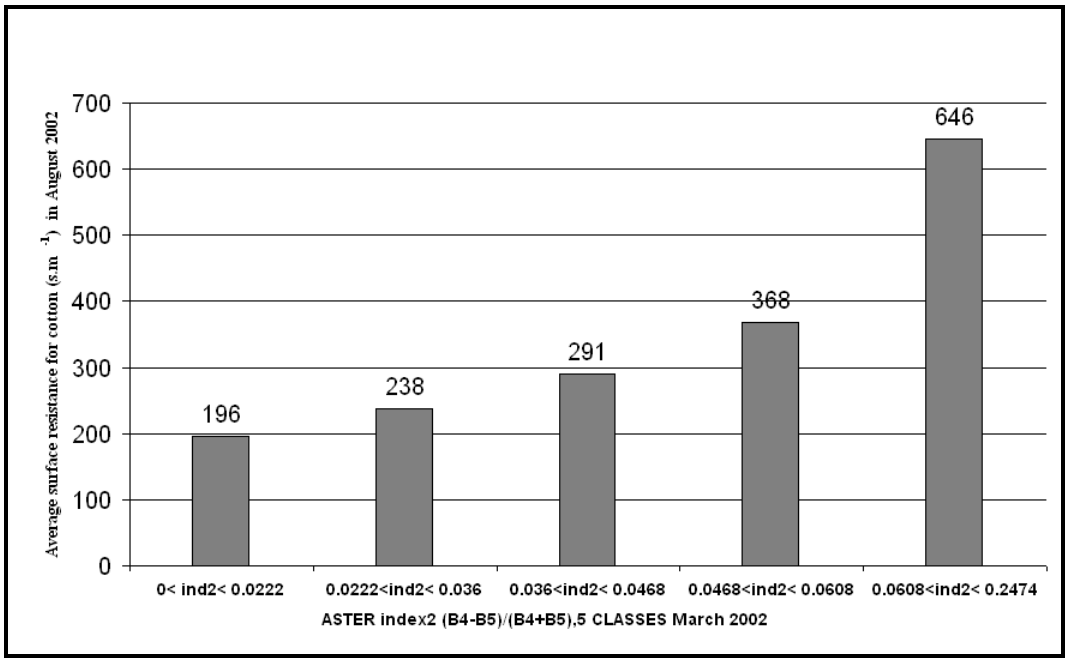

Figure 5.14 The average surface resistance in August within each class of index2

Figure 5.15 show further details that: the surface resistance is increasing with the increasing of the ASTER index. The light green bars present the pixels with low values of surface resistance in August (less than 177 $S.m^{-1}$). The height of these bars decreases strongly from the left to the right

The red bars present the number of pixels of high surface resistance values (above 350 $S.m^{-1}$).

The height of these red bars increases strongly, from the left to the right. This means with the increase of the index2 values in March the surface resistance of the cotton which grown over these lands increase too.

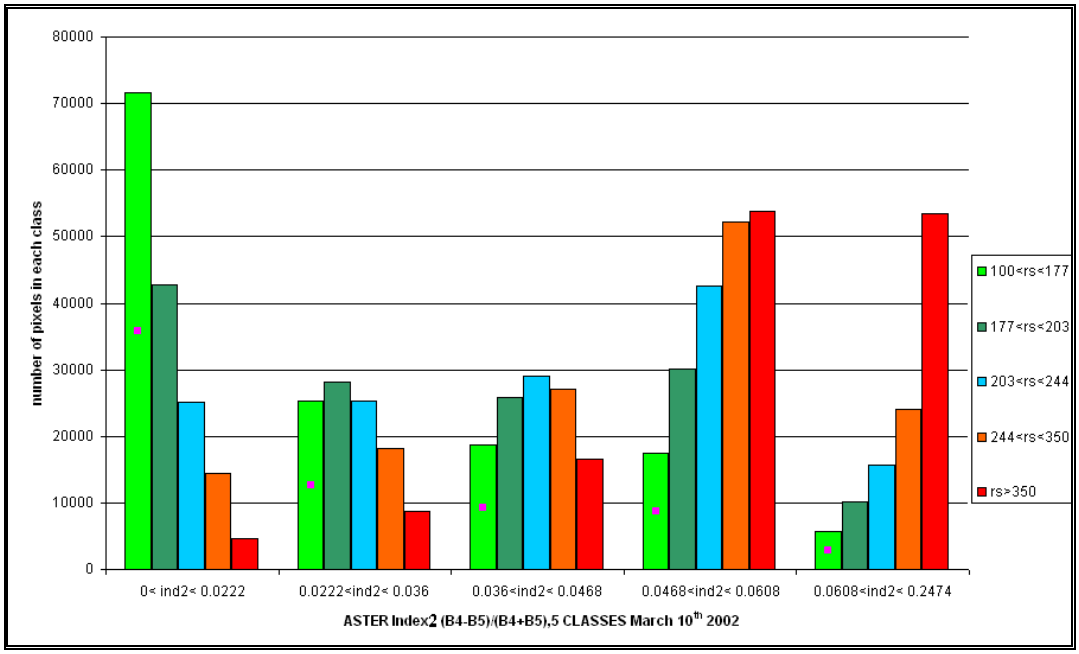

Figure 5.15 The crossing between index2 in March 10th and the surface resistance Sm^{-1} in August 24th 2002

Chapter 6 Conclusions and Recommendations

Soil salinity caused by natural or human-induced processes is a major environmental hazard. Crop growth reduction due to salinity is generally related to the soil solution osmotic potential of the root zone. As salinity levels increase, the plant must spend more energy to take up water from the same soil water content. High soil salinity can also cause nutrient imbalances, result in the accumulation of elements toxic to plants. In many areas of the world, soil salinity is the factor limiting plant growth.

The study of when, where and how soil salinization process may occur is vital to determining the sustainability of any irrigated production system. Remote sensing has been shown before to be a particularly valuable tool for obtaining relevant data on soil salinity in the irrigated area. The presence of salts at the terrain surface can be detected from remotely sensed data either directly on bare soils, with salt efflorescence and crust, or indirectly through the biophysical characteristics of vegetation as these are affected by salinity.

This study dealt with the two different methods (empirical and biophysical) using two different types of satellite data (Landsat7 ETM and ASTER) in two different crop calendar dates (immediately before and in the middle of the growing season).

The first method, the empirical, which made use of ASTER image, resulted in the following conclusions:

- The newly launched ASTER sensor has a variety of bands, and the surface reflectance of these bands is related to the soil type and soil chemical composition. A combination of ASTER bands: $\left(\frac{band4 - band3}{band4 + band3}\right)$ is perhaps useful for the detection of soil composition, such as nitrogen or iron dioxides.

- The salinity index, which is produced by ASTER bands: $\left(\frac{band4 - band5}{band4 + band5}\right)$ accurately detects overall salinity in the bare agriculture soils (R^2=0.86). This can be applied when the land is fallow.

- This study showed the possibilities to predict the success of crop growth before planting; using the ASTER bands 4 and 5, ((1.6-1.7) and (2.145-2.185) μm respectively) salinity index for bare soil. It deserves to mention here that Landsat ETM has similar bands namely 5 and 7, ((1.55-1.75) and (2.08-2.35) μm respectively) and these two bands have been

used repeatedly to detect salinity like the salinity index $\left(\frac{band5}{band7}\right)$ and the salinity index $\left(\frac{band5-band7}{band5+band7}\right)$

The second – biophysical - method is suitable for salinity detection of cropped soils. This method is built on the surface resistance of a cotton crop, which can be derived through inversion of the Penman-Monteith equation. There are nowadays several energy balance algorithms available that can map out the latent heat flux under actual conditions. In this thesis, the Surface Energy Balance Algorithm for Land has been used.

The surface resistance "r_s" is physically coupled to the osmotic potential. This study showed an adequate relationship between r_s calculated from Landsat Enhanced Thematic Mapper acquired during August, which is the central cotton season in Syria and the Electric Conductivity obtained in the field. This relation has a high correlation coefficient (R^2=0.86). When factors like water stress play no role, r_s in the middle of the growing season gives us a fair idea about soil salinity in the upper 0.75 cm of the soil column, i.e. the average root zone depth of cotton..

The relation between the surface resistance of a crop and soil salinity appear to be valid between two thresholds: the first is the value of EC at which the crop start to response to salinity, in this case 7.7 $dS.m^{-1}$ for cotton, and the second is the value of EC at which the crop gives up and dies, in this case 27 $dS.m^{-1}$.

Surface salinity processes are highly dynamic. That is why the method of detecting soil salinity should be dynamic too. Hence using multi-temporal images is a suitable way to detect the changing state of salinity, especially in irrigated areas.

The difference between the two methods

When possible, it is recommended to use both methods to assess soil salinity. The differences between the two methods are:

- The empirical method detects only the salts on the surface of the soil and gives a poor idea about the conditions below the surface, while the biophysical method indicates the condition and existence of salt in the entire soil section between the surface and the root zone. So in spite that during previous remote sensing investigation vegetation cover was supposed to be an obstacle to detect salt in the soil, this method profits from the vegetation to detect salt deeper than just the soil surface.

- The empirical method is simple and easy to apply and does not need any sophisticated calculation or any weather data. The disadvantage is that the entire relationship changes with time and location. This requires frequent field visits to adjust the coeffi-

cients. The biophysical method needs a complete algorithm to calculate advanced land surface parameters and uses many sophisticated formulas with the need for additional climate data.

- The empirical method has no threshold so as long as there is salt in the soils the reflectance will increase depending on that. For the biophysical method the matter is different. The range of salinity that can be detected depends on the crop tolerance to salinity. In this case the range is between 7.7 $dS.m^{-1}$ and 27 $dS.m^{-1}$. But this method can make use of different crops that exist in the area, to obtain a general idea on salinity conditions. . Maize is for instance sensitive to salts between EC_e=1 and 6.5 $dS.m^{-1}$

References

Ambast, S.K., 1997. Monitoring and evaluation of irrigation system performance in saline irrigated command using satellite remote sensing and gis. *Interne Mededeling, Report No.471*, DLO Winand Staring Centre, Wageningen, the Netherlands, 106 p.

Bastiaanssen, W.G.M., 1995. Regionalization of surface flux densities and moisture indicators in composite terrain: A remote sensing approach under clear skies in Mediterranean climates. Ph.D. Thesis, Landbouw Universiteie, Wageningen, The Netherlands.

Bastiaanssen, W.G.M., 1998. *Remote sensing in water resources management: The state of the art*. International Water management Institute, Colombo, Sri Lanka, 118 p.

Brena, J., H. Sanvicente and L. Pulido, 1995. Salinity assessment in Mexico. In *Use of remote sensing techniques in irrigation and drainage*, ed. A. Vidal and J. A. Sagardoy, 179-184. Water reorts 4. Rome: FAO.

Brown, J.W. and Hayward, 1956. Salt tolerance of alfalfa varieties. *Agron. J.*, vol. 48: 12-20.

Chaturvedi, L., K.R. Carver, J.C. Harlen, G.D. Hancock, F.V. Small and K.J. Dalstead, 1983. Multispectral remote sensing of saline seeps. *IEEE Transactions on Geoscience and Remote Sensing*, vol. 21(3): 239-250.

Doorenbos, J., and A.H. Kassam, 1979. Yield response to water. *FAO Irrigation and Drainage Paper No. 33*, Rome, Italy.

Dwivedi, R.S., 1969. Monitoring of salt affected soils of the Indo-Gangetic alluvial plains using principal component analysis. *International Journal of Remote Sensing,* vol.17(10):1907-1914.

FAO, 1988. Salt-affected soils and their management. *Bulletin* No. 39, FAO, Rome.

Farah, H.O., 2000. Estimation of regional evaporation under different weather conditions from satellite and standard weather data: a case study of the Naivasha Basin, Kenya. Ph.D. Thesis, Wageningen University, The Netherlands, 170 p.

Ghassemi, F., A. J. Jakeman and H.A. Nix, 1995. Salinisation of land and water resources: human causes, extent, management and case studies. Canberra, Australia: The Australian National University, Wallingford, Oxon, UK: CAB International.

Gupta, R.K. and I.P. Abrol, 1990. Salt-affected soils: Their reclamation and management for crop production. In *Advances in Soil Science*, vol.11: 223-288.

Hanan, N.P. and S.D. Prince, 1997. Stomatal conductance of west-central supersite vegetation in Hapex-sahel: measurement and empirical models. *Jour. of Hydrology*, 188-189:536-562.

Homaee, M., 1999 Root water uptake under non-uniform transient salinity and water stress. Ph.D. Thesis, Department of Environmental Sciences, Wageningen University and Research Ceater, The Netherlands, 173 p.

Hovis, W.A.Jr., 1966. Infrared spectral reflectance of some common minerals. *Applied Optics*, vol. 5(2): 245-248.

Jarvis, P.G., 1976. The interpretation of the variations in leaf water potential ansd stomatal conductance found in canopies in the field. *Phil. Trans. Royal Soc. London, Ser.B*, 273: 593-610.

Mass, E.V. and G.J. Hoffman, 1977. Crop salt tolerance and current assessment. *J. Irrigation and Drainage div*. ASCE vol.103(2):115-134.

Menenti, M., A. Lorkeers and M. vissers, 1986. An application of Thematic Mapper data in Tunisia. *ITC Journal* No. 1 : 35-42.

Metternicht, G.I. and J.A. Zinck, 2003. Remote sensing of soil salinity: potentials and constraints. *Remote Sensing of Environment,* 5812 : 1-20, article in press.

Mougenot, B. and M. Pouget, 1993. Remote sensing of salt-affected soil. In *Remote Sensing Reviews*, vol.7:241-259.

Mulders, M.A. and G.F. Epema, 1986. The Thematic Mapper: A new tool for soil mapping in arid areas. *ITC Journal* No. 1: 24-29.

Naseri, M.Y., 1998. Characterization of salt-affected soils for modeling sustainable land management in semi-arid environment; a case study in the Gorgan region, Northeast Iran. Ph.D. Thesis, Ghent University, Belgium, 321 p.

Paton, T.A.L. and A.D.S. Mangnall, 1966. Irrigation and drainage projects in the Euphrates Basin: Phase 2 Project Report-Balikh Basin March 1966. General Organization of the Euphrates project, Syrian Arab Republic, 213 p.

Paton, T.A.L. and A.D.S. Mangnall, 1967. Irrigation and drainage projects in the Euphrates Basin: Phase 2 Project Report-Balikh Basin November 1967. General Organization of the Euphrates project, Syrian Arab Republic, 121 p.

Rao, B.R., R.S. Dwivedi, L.Venkataratnam, T. Ravishankar, S.S. Thammappa, G.P. Bhargava and A.N. Singh, 1991. Mapping the magnitude of sodicity in part of Indo-Gangetic plains of Uttar Pradesh, Northern India using Landsat data. *International Journal of Remote Sensing*, vol.12: 1419-1425.

Rhoades. J.D., 1990. Soil salinity – causes and controls. In *Techniques for desert reclamation*, School of Geography University of Oxford.

Richards, L.A., 1954. Diagnosis and improvements of saline and alkali soils. U.S. Salinity Laboratory DA, US Dept. Agr. Hbk 60, 160 p.

Saha, S.K., M. Kudrat, and S.K. Bhan, 1990. Digital processing of Landsat TM data for wasteland mapping in parts of Aligarh District, Uttar Pradesh, India. *International Journal of Remote Sensing,* vol.11: 485-492.

Shalhevet, J., P. Reiniger and D. Shimshi, 1969. Peanut response to uniform and non-uniform soil salinity. *Agron. J.*, vol.61: 384-387.

Sharma, R.C. and G.P. Bhargava, 1988. Landsat imagery for mapping saline soils and wet lands in north-west India. *International Journal of Remote Sensing*, vol. 9: 39-44.

Singh, R.P., and S.K. Srivastav, 1990. Mapping waterlogged and salt affected soils using microwave radiometers. *International Journal of Remote Sensing*, vol. 11: 1879-2592.

Smedema, L.K. and K. Shiati, 2002. Irrigation and salinity: a perspective review of the salinity hazards of irrigation development in the arid zone. *Irrigation and Drainage System*, vol. 16(2):

Smedema, L.K., 1993. Salinity control of irrigated land. In *Use of remote sensing techniques in irrigation and drainage*: proceedings of the expert consultation, Montpellier, France, 2-4, November 1993. FAO, 141-150.Steven, M.D., J. Malthus, F.M. Jaggard and B. Andrieu, 1992. Monitoring responses of vegetation to stress . In *Remote sensing from research to operation : proceeding of the 18th Annual conference of the remote sensing Society, University of Dundee*, 15-17 September 1992, ed. A. P. Cracknell and R. A. Vaughan, 369-377. Nottingham, U.K.: Remote Sensing Society.

Szabolcs, I., 1979. Review of research on salt-affected soils. *Nature Resource Res.*, vol. 15:137.

Szabolcs, I., 1985. Salt-affected soil as world problem. In *1st Symposium on Reclamation of Salt-Affected Soil*, China, 8-12 May 1985:30-47.

Szabolcs, I., 1987. The global problems of salt-affected soils. *Acta Agronomica Hungarica*, vol 36:159-172.

Vidal, A., P. Maure, H. Durand and P. Strosser, 1996. Remote sensing applied to irrigation system management: Example of Pakistan. In *EURISY Colloquium: Satellite Observation for sustainable development in the Mediterranean Area*, 132-142. Paris: Promotion of Education and information Activities for the Advancement of Space Technology and its Application in Europe.

Vincent, B., A. Vidal, D. Tabbet, A. Baqri and M. Kuper, 1996. Use of satellite remote sensing for the assessment of water logging or salinity as an indication of the performance of drained systems. In *Evaluation of performance of subsurface drainage systems: 16th Congress on Irrigation and Drainage, Cairo, Egypt, 15-22 September 1996,* ed. B. Vincent, 203-216. New Delhi: International Commission on Irrigation and drainage.

Zinck, J. A. (2001). Monitoring salinity from remote sensing data. In *Proceedings of the 1st Workshop of the EARSeL Special Interest Group on Remote Sensing for Developing Countries*, ed. R. Goossens, & B. M. De Vliegher, 359– 368. Belgium: Ghent University.

Zuluaga, J.M., 1990. Remote sensing applications in irrigation management in Mendoza, Argentina. In *Remote sensing in evaluation and management of irrigation*, ed M. Menenti, 37-58. Mendoza, Argentina: Instituto Nacional de Ciencia y Técnicas Hídricas.

Appendices

Appendix A – Soil EC and pH Analysis

The procedure of analysis went through these steps:

1. Drying the soil samples in hot air oven under temperature of 60-70 °C for 24 hours.
2. Grinding the dried soil samples by a mortar and
3. Sieving the obtained powder by the US standard sieve of pore diameter 0.5 mm.
4. Mixing 200 ml of distilled water with 40 g of the sieved soil. The bottle of the mixture was shaken for 10 minutes by an electrical shaker to dissolve salt. Leaving the mixture still overnight so the soil would fully imbibe the water and the readily soluble salts would dissolve completely.
5. Filtering the aqueous solution by suction through Buckner funnel connected to a vacuum pump.
6. Measuring the extracted water for EC by standard conductance meter reported as decisiemens per meter ($dS.m^{-1}$) at 25 °C and pH meter measured pH.

Appendix B Soil Moisture Analysis

The procedure of moisture analysis went through the following steps:

1. Weighing both the metal ring (of a verified weight) and the soil in it. The total weight was recorded as wet weight.
2. Drying it in hot air oven at 105°C for 24 hours and leaving it to cool in desiccator.
3. Weighting it again and recording as dry weight
4. Calculating the soil moisture in percentage by the following formula:

$$\%\, moisture = \frac{wet\ weight - dry\ weight}{wet\ weight - ring\ weight} * 100$$

Appendix C – Raw Field Data

I	ID	X	Y	MOIST1	MOIST2	MOIST3	MOIST average	EC5_1	EC5_2	EC5_3	EC5 average	landcover	HEALTH	SALT	REMARKS
1	1	490088	4001173	29.93	28.36		29.15	0.350	0.370			cotton	perfect		
2	2	490350	4001312	18.51			18.51	8.340			8.340	bare(cotton)	bare		
3	3	490672	4001167	23.95			23.95	2.124			2.124	shawk+yellow weat			
4	2	490886	4001895	21.48	29.93	26.91	25.71	2.420	2.446	4.951		cotton	below-mid		
5	3	492388	4003119	31.27	30.99		31.13	5.528	7.734			cotton	very bad	clear	very bad land
6	4	494901	4002827	33.97	22.90	29.69	28.44	1.960	2.006	2.020		cotton	below-mid		irrigated
7	7	495985	4002727	14.18			14.18	0.960			0.960	ashwak			
8	5	496613	4004354	28.64	30.82		29.73	9.000	7.031			cotton	bad	cristal	very bad land--high moisture
9	6	495458	4004791	21.96	24.00		22.98	3.145	2.810			cotton	bad		bare spot inside the field
10	7	495485	4005872	35.89	29.31		32.60	0.515	0.500			cotton	good		
11	8	492972	4005429	34.67	34.69		34.68	3.000	2.370			cotton	mid	cristal	irrigated --short plant
12	9	492610	4004969	34.15	31.89		33.02	5.641	4.555			cotton	bad		weak density
13	10	492153	4004292	34.08	36.41	34.98	35.25	3.003	2.898	1.870		cotton	bad		diversity in density
14	14	490698	4005023					8.900			8.900	bare			
15	11	490991	4004240	21.73	25.76	24.67	23.75	0.810	2.400	2.273		cotton	over-mid	light distribut	
16	16	491479	4006499	5.48			5.48	0.284			0.284	ashwak			wheat between ashwak
17	17	492542	4007350	5.17			5.17	3.300			3.300	bare		cristal	beside the canal
18	12	493153	4007228	29.48	26.04	27.63	27.76	2.560	1.590	2.359		cotton	mid		ashwak
19	13	493665	4007517	31.38	27.94		29.66	1.690	2.501			cotton	below-mid		salinity + ashwak
20	14	496198	4008276	28.99	25.89		27.44	0.860	0.260			cotton	good		
21	15	497899	4007865	46.32	31.42		38.87	0.530	0.320			cotton	good		
22	16	498989	4006636	26.43	25.70		26.07	0.185	0.200			cotton	good		being irrigated
23	23	500464	4005958	6.40			6.40	0.185			0.185	harvested wheat			north the canal
24	17	500882	4004409	31.83	27.42		29.63	0.290	0.360			cotton	good		
25	25	500525	4004309	5.37			5.37	0.450			0.450	mafloha			some ashwak
26	18	500989	4001773	29.32	28.14		28.73	0.370	0.275			cotton	good		
27	19	501019	4000580	32.27	29.83		31.05	0.821	1.120			cotton	good		
28	20	503338	3999198	39.99	34.99		37.49	0.350	1.290			cotton	good		
29	21	503354	3997567	40.30	33.59		36.95	1.570	2.150			cotton	mid	light	salinity
30	22	496415	4000249	30.68	33.69		32.19	0.638	0.530			cotton	good		
31	31	497261	4000602	10.76			10.76	5.000			5.000	harvested wheat			organic matter
32	32	497364	4001509	11.76			11.76	17.000			17.000	bare		gipsum	tall athry
33	23	497497	4001731	43.45	40.24		41.85	4.000	3.558			cotton	bad		low land water log
34	24	497811	4005243	23.04	22.59		22.82	0.760	0.530			cotton			
35	25	498199	4005940	30.41	27.24		28.83	0.374	1.040			cotton	good		with vegitables

I	ID	X	Y	MOIST1	MOIST2	MOIST3	MOIST average	EC5_1	EC5_2	EC5_3	EC5 average	landcover	HEALTH	SALT	REMARKS
36	26	498777	4003709	27.52	27.17		27.35	0.349	1.900			cotton	good	light	
37	27	497811	4001415	16.04	34.13	26.35	25.09	4.200	3.850	3.963		cotton	bad	clear	
38	28	497775	4001083	35.84	33.19	31.92	34.52	1.740	2.069	1.312		cotton			
39	29	494683	3999940	37.27	32.50	33.58	34.89	0.872	2.260	1.732		cotton	mid	light	
40	40	494236	4000038	16.91			16.91	10.300			10.300	bare			
41	30	494279	4000211	30.73	31.20		30.97	5.280	4.297			cotton	very bad		bambo high watertable
42	42	493517	4000173	14.44			14.44	7.070			7.070	mafloha			
43	31	493074	4000692	24.35	23.51		23.93	3.350	3.016			cotton			
44	32	477126	3979778	34.76	30.10	31.18	32.01	0.280	0.280	0.272		cotton	good	on the borders	on borders bad no drain but in the drained area very good
45	45	477702	3981527	7.65			7.65	0.202			0.202	harvested wheat			
46	46	478070	3983260	29.70	25.80		27.75	0.218	0.230		0.224	yellow maize	good and bad		there is bad spots
47	33	478327	3984672	31.18	30.98	30.27	30.81	0.186	0.230	0.209		cotton	good		bad on the borders
48	48	479686	3986198	33.93	31.62		32.78	0.185	0.255		0.220	yellow maize	good		bad spots
49	34	480814	3989108	25.66	25.23	25.59	25.49	0.220	0.202	0.215		cotton	good		
50	50	478043	3990046	9.66			9.66	14.200			14.200	bare(salinity)			
51	35	477289	3988717	28.24	27.87	29.55	28.55	0.285	0.231	0.635		cotton	good		irrigated soon
52	52	477376	3988855	20.01	22.32		21.17	11.210	7.600		9.405	shawk		full of	
53	36	475962	3989152	22.42	16.87	22.79	20.69	4.578	1.927	1.390		cotton	mid		dry soil
54	37	475098	3988304	25.68	27.18	27.11	26.66	0.235	0.870	0.541		cotton	good-mid		on the left of road good cotton, on the left big area of water.log
55	55	475224	3988409					24.500			24.500	shawk			
56	56	476378	3987723	15.60	20.09		17.85	6.400	4.020		5.210	ashwak			has been used long time ago maybe 2-3 years(full of shawk)
57	57	477093	3987408	1055.00			1055.00	2.816			2.816	cut hoor			
58	38	475746	3989479	25.10	24.80	21.28	23.73	0.223	0.223	0.240		cotton	good		very exelent land avesting first time of two
59	59	475832	3989451	11.09			11.09	7.200			7.200	shawk			high density
60	60	477329	3991192	4.33			4.33	0.300			0.300	bare			was sha'eer no irrigated
61	61	477975	3991402	14.76			14.76	80.580			80.580	shawk		full	was used very high salinity and shawk
62	62	478592	3992036	7.45			7.45	0.600			0.600	maflwha(khrbana)		yes	covered drain malfunction (not used)
63	39	479173	3992285	20.14	24.10	25.87	23.37	0.200	0.269	0.222		cotton	over mid		red cotton leaves dry land har-
64	40	480640	3991990	27.30	25.68	27.37	26.78	0.230	0.280	0.350		cotton	mid goood		

I	ID	X	Y	MOIST1	MOIST2	MOIST3	MOIST average	EC5_1	EC5_2	EC5_3	EC5 average	landcover	HEALTH	SALT	REMARKS
65	65	480498	3992045	5.20			5.20	0.523			0.523	maflwha		clear	not working covered drain
66	66	481713	3992477	6.42			6.42	0.280			0.280	old cotton			cotton last year
67	41	482160	3993752	23.27	23.25	27.39	24.64	0.500	0.540	0.550		cotton	good		
68	42	482646	3995248	25.72	25.10	26.97	25.93	0.280	0.280	0.300		cotton	good		harvesting
69	69	482837	3995968	61.80			61.80	0.230			0.230	bare maflwha			
70	43	481007	3996224	25.99	25.48	25.91	25.79	0.600	0.270	0.448		cotton	mid to good		with bad grass
71	44	481741	3998632	22.67	27.14	30.46	26.76	1.689	1.940	1.802		cotton	mid to bad	light	sand in the depth
72	45	483150	3999558	29.42	31.70	35.77	32.30	3.160	2.540	2.624		cotton		clear high	
73	46	483669	4001545	26.42	28.40	31.36	28.73	1.380	1.300	1.355		cotton			beside the field salty land
74	47	484742	4000479	24.18	25.52	28.57	26.09	0.307	0.285			cotton	good		good
75	48	486000	4001873	25.13	26.00	28.15	26.43	0.450	0.970			cotton	good		
76	76	486003	4001634	12.86			12.86	0.280			0.280	watermelon			
77	49	486537	3989146	13.95	19.01	21.95	18.30	0.250	0.520	0.385		cotton	good to mid		defrentiated
78	78	486590	3989390	12.31			12.31	2.705			2.705	watermelon	good		gepsum
79	79	487873	3990725	21.99			21.99	34.520			34.520	shawk(sobakh)			wide area of shawk
80	50	488459	3991560	25.24	27.86	27.31	26.80	0.820	0.713	0.719		cotton	good		
81	51	494697	3991884	24.78	22.45	22.65	23.29	1.377	2.025	1.598		cotton	good to mid	yes	
82	52	496882	3991617	23.75	26.63	27.53	25.97	0.633	0.561	0.629		cotton	good	on borders	wide field
83	83	498137	3999872	7.79			7.79	1.526			1.526	mafloha			
84	53	499939	3999949	21.71	24.25	27.42	24.46	0.577	1.191	0.891		cotton	good		
85	54	499801	3997913	29.77	28.59	29.38	29.25	0.519	1.790	1.453		cotton	good		very wide area
86	55	491409	3997698	20.33	22.35	25.13	22.60	0.246	0.249	0.371		cotton	mid to good	on borders	
87	56	487196	3994343	17.88	21.29	30.45	23.21	0.690	1.730	1.670		cotton	good		carbon in the middle
88	57	487244	3996683	16.69	21.21	22.51	20.14	1.041	2.231	2.501		cotton	bad		gepsum
89	58	498347	3991612	17.38	24.11	25.64	22.38	0.335	0.270	0.314		cotton	mid to good		
90	90	498505	3991602	18.77			18.77	11.930			11.930	bare+shawk			clear sobakh
91	91	498694	3992522	16.49			16.49	3.350			3.350	bare			absulute sobakh
92	59	500000	3991601	12.66	21.12	24.45	19.41	1.214	1.023	1.143		cotton	good		
93	93	493760	3999054	19.29			19.29	19.750			19.750	bare+shawk			
94	60	490961	3998644	10.92	9.58		10.25	0.652	0.602			cotton	good		hard soil hard to dig
95	61	490425	3996917	13.34	20.19	27.13	20.22	5.094	6.995	6.031		cotton			
96	96	490337	3996328	17.17			17.17	5.580			5.580	watermelon			
97	97	486660	3997596	21.66			21.66	0.485			0.485	mafloha			
98	98	483905	4000284	20.92			20.92	9.330			9.330	bare			

Appendix D – Field Data for Moisture, EC5 and ECe for cotton fields only.

ID	GPS	X	Y	MOIST1	MOIST2	MOIST3	MOIST average	EC5_1	EC5_2	EC5_3	ECe1	ECe2	ECe3	ECe average	HEALTH	SALT
1	58	490088	4001173	29.93	28.36		29.15	0.350	0.370		1.850	1.930		1.890	perfect	
2	63	490886	4001895	21.48	29.93	26.91	25.71	2.420	2.446	4.951	13.310	15.654	31.684	20.216	below-mid	
3	68	492388	4003119	31.27	30.99		31.13	5.528	7.734		35.378	49.500		42.439	very bad	clear
4	72	494901	4002827	33.97	22.90	29.69	28.44	1.960	2.006	2.020	10.780	11.033	11.110	10.974	below-mid	
5	75	496613	4004354	28.64	30.82		29.73	9.000	7.031		57.600	45.000		51.300	bad	cristal
6	77	495458	4004791	21.96	24.00		22.98	3.145	2.810		20.129	17.985		19.057	bad	
7	78	495485	4005872	35.89	29.31		32.60	0.515	0.500		2.510	2.450		2.480	good	
8	81	492972	4005429	34.67	34.69		34.68	3.000	2.370		19.200	15.168		17.184	mid	cristal
9	84	492610	4004969	34.15	31.89		33.02	5.641	4.555		36.100	29.150		32.625	bad	
10	85	492153	4004292	34.08	36.41	34.98	35.25	3.003	2.898	1.870	19.220	18.544	10.285	16.016	bad	
11	90	490991	4004240	21.73	25.76	24.67	23.75	0.810	2.400	2.273	3.690	13.200	12.502	9.797	over-mid	light distribut
12	99	493153	4007228	29.48	26.04	27.63	27.76	2.560	1.590	2.359	16.384	8.745	12.974	12.701	mid	
13	101	493665	4007517	31.38	27.94		29.66	1.690	2.501		9.295	16.006		12.651	below-mid	
14	105	496198	4008276	28.99	25.89		27.44	0.860	0.260		3.890	1.490		2.690	good	
15	107	497899	4007865	46.32	31.42		38.87	0.530	0.320		2.570	1.730		2.150	good	
16	117	498989	4006636	26.43	25.70		26.07	0.185	0.200		1.190	1.250		1.220	good	
17	126	500882	4004409	31.83	27.42		29.63	0.290	0.360		1.610	1.890		1.750	good	
18	128	500989	4001773	29.32	28.14		28.73	0.370	0.275		1.930	1.550		1.740	good	
19	130	501019	4000580	32.27	29.83		31.05	0.821	1.120		3.734	4.930		4.332	good	
20	133	503338	3999198	39.99	34.99		37.49	0.350	1.290		1.850	5.610		3.730	good	
21	135	503354	3997567	40.30	33.59		36.95	1.570	2.150		8.635	11.825		10.230	mid	light
22	147	496415	4000249	30.68	33.69		32.19	0.638	0.530		3.002	2.570		2.786	good	
23	157	497497	4001731	43.45	40.24		41.85	4.000	3.558		25.600	22.770		24.185	bad	
24	173	497811	4005243	23.04	22.59		22.82	0.760	0.530		3.490	2.570		3.030		
25	177	498199	4005940	30.41	27.24		28.83	0.374	1.040		1.946	4.610		3.278	good	
26	194	498777	4003709	27.52	27.17		27.35	0.349	1.900		1.846	10.450		6.148	good	light
27	199	497811	4001415	16.04	34.13	26.35	25.09	4.200	3.850	3.963	26.880	24.640	25.361	25.627	bad	clear
28	200	497775	4001083	35.84	33.19	31.92	34.52	1.740	2.069	1.312	9.570	11.380	5.698	8.883		
29	204	494683	3999940	37.27	32.50	33.58	34.89	0.872	2.260	1.732	3.938	14.464	9.524	9.309	mid	light
30	207	494279	4000211	30.73	31.20		30.97	5.280	4.297		33.792	27.500		30.646	very bad	
31	210	493074	4000692	24.35	23.51		23.93	3.350	3.016		21.440	19.305		20.373		
32	218	477126	3979778	34.76	30.10	31.18	32.01	0.280	0.280	0.272	1.570	1.570	1.538	1.559	good	on the borders
33	231	478327	3984672	31.18	30.98	30.27	30.81	0.186	0.230	0.209	1.194	1.370	1.284	1.283	good	

ID	GPS	X	Y	MOIST1	MOIST2	MOIST3	MOIST average	EC5_1	EC5_2	EC5_3	ECe1	ECe2	ECe3	ECe average	HEALTH	SALT
34	243	480814	3989108	25.66	25.23	25.59	25.49	0.220	0.202	0.215	1.330	1.258	1.309	1.299	good	
35	250	477289	3988717	28.24	27.87	29.55	28.55	0.285	0.231	0.635	1.590	1.374	2.990	1.985	good	
36	255	475962	3989152	22.42	16.87	22.79	20.69	4.578	1.927	1.390	29.300	10.600	7.645	15.848	mid	
37	261	475098	3988304	25.68	27.18	27.11	26.66	0.235	0.870	0.541	1.390	3.930	2.614	2.645	good-mid	
38	274	475746	3989479	25.10	24.80	21.28	23.73	0.223	0.223	0.240	1.342	1.342	1.409	1.364	good	
39	290	479173	3992285	20.14	24.10	25.87	23.37	0.200	0.269	0.222	1.250	1.526	1.338	1.371	over mid	
40	309	480640	3991990	27.30	25.68	27.37	26.78	0.230	0.280	0.350	1.370	1.570	1.850	1.597	mid goood	
41	326	482160	3993752	23.27	23.25	27.39	24.64	0.500	0.540	0.550	2.450	2.610	2.650	2.570	good	
42	331	482646	3995248	25.72	25.10	26.97	25.93	0.280	0.280	0.300	1.570	1.570	1.650	1.597	good	
43	336	481007	3996224	25.99	25.48	25.91	25.79	0.600	0.270	0.448	2.850	1.530	2.240	2.207	mid to good	
44	349	481741	3998632	22.67	27.14	30.46	26.76	1.689	1.940	1.802	9.290	10.670	9.912	9.957	mid to bad	light
45	362	483150	3999558	29.42	31.70	35.77	32.30	3.160	2.540	2.624	20.224	16.256	16.792	17.757		clear high
46	370	483669	4001545	26.42	28.40	31.36	28.73	1.380	1.300	1.355	5.970	5.650	5.870	5.830		
47	376	484742	4000479	24.18	25.52	28.57	26.09	0.307	0.285		1.678	1.590		1.634	good	
48	381	486000	4001873	25.13	26.00	28.15	26.43	0.450	0.970		2.250	4.330		3.290	good	
49	386	486537	3989146	13.95	19.01	21.95	18.30	0.250	0.520	0.385	1.450	2.530	1.988	1.989	good to mid	
50	398	488459	3991560	25.24	27.86	27.31	26.80	0.820	0.713	0.719	3.730	3.302	3.326	3.453	good	
51	404	494697	3991884	24.78	22.45	22.65	23.29	1.377	2.025	1.598	5.958	11.138	8.790	8.629	good to mid	yes
52	408	496882	3991617	23.75	26.63	27.53	25.97	0.633	0.561	0.629	2.982	2.694	2.966	2.881	good	on borders
53	423	499939	3999949	21.71	24.25	27.42	24.46	0.577	1.191	0.891	2.758	5.214	4.014	3.995	good	
54	429	499801	3997913	29.77	28.59	29.38	29.25	0.519	1.790	1.453	2.526	9.845	6.262	6.211	good	
55	431	491409	3997698	20.33	22.35	25.13	22.60	0.246	0.249	0.371	1.434	1.446	1.934	1.605	mid to good	on borders
56	440	487196	3994343	17.88	21.29	30.45	23.21	0.690	1.730	1.670	3.210	9.515	9.185	7.303	good	
57	443	487244	3996683	16.69	21.21	22.51	20.14	1.041	2.231	2.501	4.614	12.271	16.006	10.964	bad	
58	1	498347	3991612	17.38	24.11	25.64	22.38	0.335	0.270	0.314	1.790	1.530	1.706	1.675	mid to good	
59	37	500000	3991601	12.66	21.12	24.45	19.41	1.214	1.023	1.143	5.306	4.542	5.020	4.956	good	
60	80	490961	3998644	10.92	9.58		10.25	0.652	0.602		3.058	2.856		2.957	good	
61	87	490425	3996917	13.34	20.19	27.13	20.22	5.094	6.995	6.031	32.600	44.770	38.598	38.656		

Appendix E – Piezometric data

No.	x	y	z	17/6 - 20/5		Jun-Jul 2001		27-8/6-9-2001		25-11/31-12-2001		25-4/8-5-2002		20-7/28-7-2002	
				No.	x	No.	x	No.	x	No.	x	No.	x	No.	x
40	24 410.44	214 224.47	275.609	40	3.75	40	3.6	40	3.72	40	4.22	40	4.02	40	3.75
41	23 184.20	214 180.18	277.297	41	2.32	41	2.2	41	2.07	41	2.12	41	2.06	41	1.85
42	26 415.22	213 318.82	279.035	42	2.2	42	2.3	42	2.11	42	2.79	42	2.77	42	2.96
43	25 509.53	213 311.67	277.762	51	2.15	51	2.63	51	2.45	51	3.55	51	2.75	51	3.16
51	25 242.85	217 198.26	269.926	52	3.05	52	4	52	4.8	52	5.58	52	4.77	52	5.55
52	24 259.00	216 909.83	270.008	54	2.45	54	2.85	54	2.35	54	3.7	54	2.84	54	2.67
53	23 605.05	216 845.07	270.513	60	2	60	1.95	60	2.12	60	2.85	60	2.65	60	2.9
54	22 763.63	216 710.79	270.587	61	1.85	61	1.5	61	1.8	61	2.04	61	1.98	61	1.7
59	25 276.45	215 796.70	271.357	62	2	62	2.14	62	2.15	62	2.73	62	1.78	62	2.33
60	24 422.84	215 648.96	272.315	65	3.25	66	1.84	66	2.05	66	1.83	66	1.21	66	2.12
61	23 779.72	215 875.08	271.957	66	2.77	67	3.48	67	3.95	67	3.97	67	3.74	67	2.9
62	22 875.85	215 413.83	271.244	67	3.48	68	2.36	68	3.02	68	2.92	68	2.88	68	2.15
63	26 790.29	215 587.78	270.727	68	2.96	78	10.71	78	10.81	78	10.76	78	10.88	78	11
64	27 180.56	215 284.30	270.962	74	2.4	78	2.75	78	2.68	78	3.25	78	2.31	78	2.25
65	26 239.16	215 074.84	273.077	77	10.5	81	1.15	81	1.6	81	1.58	81	1.04	81	1.58
66	24 455.02	214 788.55	273.512	78	8.45	82	2.37	82	1.84	82	2.7	82	1.85	82	1.99
66	26 192.82	215 574.97	270.739	78	2	86	2.2	86	1.85	86	3.15	86	2.94	86	2.39
67	23 644.54	214 639.57	274.785	81	1.38	87	3.08	87	2.84	87	3.3	87	3.06	87	3.01
68	22 888.84	214 811.20	272.825	82	1.06	91	5.34	91	9.15	91	10.64	91	3.03	91	2.19
69	21 929.58	214 986.45	272.833	86	2.5	96	2.52	96	1.16	96	2.37	96	1.11	96	1.79
72	20 992.48	215 733.05	270.755	87	2.85	101	2.2	101	1.85	101	3.02	101	1.58	101	2.1
73	20 104.01	215 604.13	270.474	91	5.5	101	1.85	101	1.31	101	2.1	101	1.56	101	2.08
74	19 187.63	215 480.65	270.463	92	3	102	2.25	102	2.82	102	2.87	102	2.3	102	1.86
75	18 288.36	215 336.46	269.59	93	8.16	104	2.02	104	1.72	104	0.7	104	1.35	104	0.92
76	17 293.76	215 250.09	270.355	94	2.1	105	2.3	105	1.1	105	2.4	105	1	105	1.12
77	16 481.41	215 239.29	270.349	96	1.35	108	2.1	108	2.27	108	3.1	108	2.4	108	1.68
78	22 228.65	216 633.54	269.93	98	10.15	109	3.2	109	1.54	109	4.76	109	2.52	109	2.87
78	14 993.55	214 065.13	268.91	101	2	110	2.7	110	3.02	110	3.29	110	2.74	110	2.2
79	21 543.86	216 561.75	270.01	102	2.36	112	2.05	112	3.03	112	3.29	112	2.31	112	2.16
80	20 860.94	216 467.72	270.765	103	2.34	114	1.85	114	1.86	114	1.79	114	1.85	114	1.78
81	19 986.08	216 345.61	270.466	104	1.72	115	2.08	115	1.75	115	2.2	115	1.63	115	1.98
82	19 068.23	216 238.69	271.031	105	1.01	116	3.16	116	2.82	116	4.35	116	3.11	116	2.83
83	18 177.19	216 116.96	270595	108	2.43	117	2.1	117	1.9	117	2.5	117	1.91	117	2.1
86	22 033.92	217 429.78	271.89	109	3.25	118	1.6	118	1.02	118	2.3	118	1.38	118	1.14
87	21 528.34	217 370.80	271.485	110	2.58	119	2.65	119	2.83	119	3.28	119	2.42	119	1.88
88	20 755.78	217 258.57	270.799	112	2.45	120	2.5	120	3.25	120	3.13	120	2.64	120	1.88
89	19 850.45	217 143.19	271.354	114	1.9	121	2.35	121	2.96	121	1.93	121	1.52	121	1.56
90	18 985.68	217 029.20	271.482	115	1.95	122	2.5	122	3.1	122	1.59	122	1.22	122	1.98
91	18 125.18	216 922.17	271.137	116	3.77	124	2.75	124	1.75	124	3.36	124	2.52	124	2.5
92	17 111.96	216 794.27	271.844	117	2.12	125	2	125	1.8	125	1.85	125	1.79	125	2.12
93	16 246.43	216 674.31	271.724	118	1.65	126	3.8	126	2.65	126	5.8	126	5.46	126	1.71
94	21 906.08	218 255.66	272.969	119	2.55	127	3.5	127	3.35	127	3.86	127	3.14	127	3.72
95	21 473.09	218 160.40	272.509	120	2.4	128	2.65	128	3	128	2.89	128	1.28	128	1.9
96	20 688.80	218 050.60	272.075	121	1.93	129	2.68	129	3.02	129	2.75	129	2.43	129	2.28
97	19 754.24	217 924.68	271.726	122	1.23	130	2.63	130	2.8	130	3.65	130	1.21	130	1.1
98	18 886.55	217 820.33	271.661	124	2.85	131	1.64	131	1.36	131	2.5	131	1.32	131	1.42
99	17 977.66	217 709.68	271.332	125	2.46	132	2.73	132	2.6	132	3.75	132	2.58	132	2.85
100	16 982.71	217 576.49	271.922	126	4.34	134	2.4	134	2.37	134	3.33	134	1.74	134	2.34
101	21 821.21	219 014.58	273.542	127	3.31	136	4.1	136	4.15	136	4.57	136	4.27	136	4.4
101	16 127.74	217 440.79	272.411	128	2.4	137	3.47	137	3.11	137	3.57	137	2.07	137	2.97
102	21 306.10	218 961.37	273.135	129	2.37	138	2.6	138	2.23	138	3.3	138	2.5	138	2.75

No.	x	y	z	17/6 - 20/5		Jun-Jul 2001		27-8/6-9-2001		25-11/31-12-2001		25-4/8-5-2002		20-7/28-7-2002	
103	20 547.42	218 853.20	273.308	130	1.09	139	2.65	139	2.43	139	3.1	139	2.35	139	2.6
104	19 629.35	218 696.40	272.417	131	2.32	140	2	140	1.62	140	2.1	140	1.65	140	2.02
105	18 769.79	218 611.55	272.046	132	2	141	2.62	141	3.12	141	2.9	141	1.8	141	2.21
106	17 878.14	218 500.67	272.439	134	2.13	142	2.2	142	1.78	142	2.71	142	1.81	142	2.33
107	16 901.74	218 379.11	272.976	136	4.14	143	2.6	143	2.82	143	3.62	143	2.61	143	2.69
108	16 063.44	218 263.28	272.863	137	3.05	144	3	144	2.6	144	3.83	144	2.8	144	2.85
109	22 009.56	219 846.27	274.681	138	2.4	145	2.56	145	2.13	145	3.23	145	2.04	145	1.97
110	21 244.76	219 755.43	273.691	139	2.61	148	1.88	146	3.7	146	4.85	146	4.12	146	3.85
111	20 430.41	219 633.39	273.505	140	2.1	149	1.6	148	1.72	148	2.2	148	1.39	148	2.02
112	19 532.22	219 502.52	273.141	141	2.14	151	2.5	149	1.82	149	2.16	149	1.47	149	1.9
113	18 643.00	219 406.19	272.991	142	2.1	152	3.35	151	2.76	151	3.55	151	2.7	151	2.85
114	17 760.42	219 292.87	274.179	143	2.72	153	3.15	152	3.08	152	4.2	152	3.23	152	3.28
115	16 782.42	219 165.97	273.823	144	3.25	154	4.15	153	3.2	153	4.45	153	2.95	153	3.18
116	15 918.18	219 031.15	274.04	145	3	156	3	154	4.04	154	4.75	154	3.91	154	2.05
117	22 507.31	220 722.89	276.775	146	4.1	159	3.98	156	1.67	156	2.58	156	1.92	156	2.01
118	21 879.61	220 641.18	275.119	147	4	160	5.82	159	4.23	159	4.34	159	4.01	159	3.98
119	21 153.35	220 546.04	274.173	148	1.48	161	4.1	160	4.65	160	6.7	160	5.76	160	5.52
120	20 347.04	220 438.50	273.815	149	2.02	162	4.15	161	3.84	161	4.7	161	4	161	4.45
121	19 430.51	220 302.78	275.147	151	2.9	164	2.78	162	4.4	162	4.76	162	4.43	162	4.38
122	18 533.41	220 199.77	274.249	152	3.6	165	3.4	164	2.4	164	3.4	164	2.07	164	3.15
123	17 648.96	220 082.14	275.242	153	3.44	168	3	165	3.43	165	3.53	165	3.4	165	3.28
124	16 680.95	219 896.78	274.434	154	3.52	169	1.85	168	3.32	168	3.83	168	3.16	168	3.22
125	15 824.14	219 844.40	274.437	155	1.25	170	1.6	169	1.8	169	2.43	169	2.04	169	1.8
126	23 341.51	221 207.07	279.155	156	1.6	172	2.27	170	1.35	170	2	170	1.73	170	1.69
127	22 402.25	221 504.25	278.719	159	4.02	176	1.62	172	1.98	172	2.62	172	2.2	172	2.13
128	21 789.15	221 422.79	276.584	160	5.94	177	1.74	176	0.82	176	2.28	176	1.64	176	1.9
129	21 025.61	221 336.41	275.942	161	4.35	178	1.8	177	2.3	177	3.14	177	2.27	177	2.48
130	20 241.53	221 225.15	275.541	162	4.68	179	2.02	178	1.85	178	3.12	178	2.51	178	2.88
131	19 322.34	221 098.89	275.825	164	3.14	181	1.65	179	1.95	179	2.94	179	2.12	179	2.2
132	18 438.37	220 991.90	275.305	165	3.44	183	2.75	181	1.83	181	2.29	180	1.72	180	1.84
133	17 559.93	220 882.23	275.862	168	3.08	184	2.65	183	2.97	183	3.22	181	1.87	181	1.71
134	16 582.79	220 741.27	275.384	169	1.88	185	3.68	184	1.92	184	2.91	183	2.3	183	2.93
135	15 720.10	220 601.43	274.451	170	1.37	186	5.7	185	4.75	185	4.72	184	2.1	184	2.84
136	22 419.80	222 077.65	279.722	172	2.13	187	2.66	186	9.46	186	10.2	185	3.72	185	4.72
137	21 656.20	222 222.60	278.441	176	1.8	188	10.1	187	3.58	187	3.83	186	10.28	186	10.95
138	20 900.42	222 129.12	277.598	177	2.34	189	2.24	188	4	188	5.62	187	2.8	187	3.82
139	20 146.12	222 029.62	276.983	178	2.65	190	2.9	189	2.04	189	1.75	188	4.9	188	4.25
140	19 217.47	221 909.58	277.493	179	2.2	193	2.9	190	2.4	190	2.85	189	1.54	189	2.17
141	18 344.94	221 795.72	276.704	181	1.64	194	2.8	193	1.65	193	2.8	190	1.91	190	2.18
142	17 453.21	221 675.57	276.677	183	2.05	195	2.72	194	1.85	194	3.2	193	2.16	193	2.28
143	16 467.20	221 543.16	276.8	184	2.26	196	2.77	195	1.74	195	3	194	2.26	194	2.62
144	15 614.05	221 423.95	276.049	185	3.4	198	2.4	196	2.65	196	3.26	195	2.22	195	2.2
145	21 607.55	222 863.47	280.362	186	10.13	199	3.5	198	2.54	198	2.96	196	2.45	196	2.53
146	20 820.37	223 042.46	279.491	187	2.4	200	3.82	199	3.25	199	4.05	198	2.3	198	2.48
147	19 909.23	222 820.32	279.021	188	3.24	202	2.54	200	3.1	200	4.15	199	4.4	199	3.81
148	19 125.96	222 686.75	278.293	189	1.87	203	8.1	202	2.08	202	4.05	200	3.6	200	3.18
149	18 259.37	222 582.29	277.478	190	2.35	204	2.36	203	5.8	203	7.72	202	2.81	202	2.82
150	17 338.42	222 455.95	277.496	193	2.01	206	1.5	204	2.48	204	3.4	203	5.28	203	4.91
151	16 362.31	222 355.01	277.992	194	2.38	208	2.8	206	1.7	206	2.23	204	1.98	204	2.23
152	15 520.09	222 172.10	277.365	195	2.19	209	2.63	208	2.75	208	3.6	206	1.61	206	1.45
153	19 374.16	223 398.43	279.909	196	2.35	210	2.24	209	3	209	3.94	208	2.72	208	2.4
154	18 597.52	223 859.35	278.815	198	2.48	212	1.65	210	2.3	210	2.32	209	2.5	209	2.43
155	18 131.87	223 462.46	278.569	199	4.1	213	1.95	212	1.2	212	2	210	2.26	210	2.3
156	17 233.76	223 343.64	278.287	200	3.36	214	2.05	213	3.1	213	3.32	212	1.28	212	1.96
157	16 254.09	223 214.44	278.731	202	2.99	215	2.1	214	1.9	214	2.38	213	2.17	213	2.98

No.	x	y	z	17/6 - 20/5		Jun-Jul 2001		27-8/6-9-2001		25-11/31-12-2001		25-4/8-5-2002		20-7/28-7-2002	
158	15 503.15	223 124.18	278.358	203	5.84	216	1.95	215	1.64	215	3.65	214	2.15	214	1.84
159	18 005.09	224 387.98	278.429	204	2.28			216	1.86	216	2.91	215	3.17	215	1.25
160	17 131.22	224 193.22	279.546	206	1.81							216	2.73	216	2
161	16 138.25	224 060.48	279.41	208	2.45										
162	15 596.64	223 607.33	279.068	209	2.58										
163	27 924.09	216 009.94	270.263	210	2.39										
164	28 591.99	216 350.43	269.607	212	0.95										
165	27 924.44	216 799.55	270.25	213	2.24										
166	27 030.74	217 071.07	269.912	214	1.99										
168	28 749.56	215 141.83	268.82	215	2.65										
169	29 101.67	216 138.49	269.857	216	2.47										
170	30 008.16	216 864.92	272.032												
171	29 173.21	216 937.61	270.85												
172	28 554.37	216 986.13	270.305												
173	29 817.91	217 685.56	274.666												
174	28 919.00	217 751.31	272.805												
175	27 975.84	217 812.36	273.245												
176	27 070.30	217 897.28	271.161												
177	26 452.70	217 953.48	270.636												
178	25 593.57	218 036.05	274.078												
179	24 915.04	217 758.64	272.242												
180	24 168.79	217 845.07	270.915												
181	23 398.00	217 572.56	270.54												
183	33 270.50	209 620.70	264.031												
184	32 447.27	209 229.00	263.571												
185	31 806.63	208 364.02	263.171												
186	31 175.88	208 273.86	265.402												
187	31 607.81	208 992.43	263.591												
188	30 954.10	209 073.21	263.445												
189	33 879.55	210 630.55	267.35												
190	33 028.68	210 313.74	265.08												
191	32 174.46	210 025.89	266.154												
192	31 352.92	209 761.29	264.604												
193	33 600.96	211 353.54	270.907												
194	32 781.70	211 076.30	265.92												
195	31 924.95	210 788.00	266.519												
196	31 098.29	210 510.47	265.257												
197	33 047.34	211 998.61	270.112												
198	32 517.36	211 831.28	266.945												
199	31 663.73	211 544.66	268.392												
200	30 844.33	211 282.97	266.644												
201	32 314.35	212 595.82	270.8												
202	31 712.55	212 378.02	270.6												
203	30 613.99	212 044.34	266.821												
204	30 861.50	212 679.36	267.634												
206	30 905.44	213 278.41	267.382												
207	30 280.46	213 618.39	266.406												
208	29 538.81	214 323.58	266.757												
209	29 016.85	214 854.21	267.379												
210	32 180.31	213 405.52	273.984												
211	31 438.94	213 829.20	272.41												
212	30 730.54	214 337.29	271.805												
213	30 159.48	214 723.85	270.418												
214	29 569.66	215 097.06	268.808												
215	30 599.32	215 370.64	272.785												
216	30 020.65	215 760.42	271.412												